Drug Research Program
Division of Pharmaceutical Chemistry and Technology
Faculty of Pharmacy
University of Helsinki

MICROFLUIDICS AND NANOTECHNOLOGY IN PHARMACEUTICAL ANALYSIS AND DRUG METABOLISM RESEARCH

Elisa Ollikainen

DOCTORAL DISSERTATION

To be presented for public discussion, with the permission of the Faculty of Pharmacy of the University of Helsinki, in lecture hall 1041,Biocenter 2, on the 18th of October, 2019, at 12 o'clock.

Helsinki 2019

ISBN 978-951-51-5540-5 (paperback)
ISBN 978-951-51-5541-2 (PDF)
ISNN 2342-3161 (print)
ISNN 2342-317X (online)
http://ethesis.helsinki.fi

Published in
Dissertationes Scholae Doctoralis Ad Sanitatem Investigandam Universitatis Helsinkiensis

Unigrafia, Helsinki 2019

Supervisor

Docent Tiina Sikanen
Drug Research Program
Division of Pharmaceutical Chemistry and Technology
Faculty of Pharmacy
University of Helsinki
Finland

Co-supervisors

Professor Risto Kostiainen
Drug Research Program
Division of Pharmaceutical Chemistry and Technology
Faculty of Pharmacy
University of Helsinki
Finland

Professor Tapio Kotiaho
Drug Research Program
Division of Pharmaceutical Chemistry and Technology
Faculty of Pharmacy, and
Department of Chemistry
Faculty of Science
University of Helsinki
Finland

Reviewers

Docent Ari Tolonen
Admescope Ltd
Oulu, Finland

Professor James P. Landers
Department of Chemistry
University of Virginia
Charlottesville, VA, USA

Opponent

Professor Elisabeth Verpoorte
Pharmaceutical Analysis,
Groningen Research Institute of Pharmacy
Faculty of Science and Engineering
University of Groningen
The Netherlands

ABSTRACT

Drug metabolism is an important area of pharmaceutical research as it has significant effects on safety and efficacy of the therapy. Cytochrome P450 (CYP) enzymes metabolize the majority of clinically used drugs and have thus a critical role in their elimination process. Alterations in CYP activities can lead to unexpected adverse effects and toxicity (low activity), or on the other hand to complete lack of efficacy (high activity). Wide inter-individual variation in CYP activities is observed due to polymorphism as well as other individual and external factors. The emerging approach, called precision medicine, aims to increase the efficacy and safety of the treatment by considering the individual characteristic of the patient. The medication is then prescribed based on this information together with the diagnosis. Individual variation in CYP activities is one of the factors that should be considered when designing the treatment. Another aspect of precision medicine is targeted drug delivery with help of nanocarriers, which enables controlled release and accumulation of the drug at the targeted site. This approach improves the bioavailability of the drug and thus also the efficacy of the treatment, whereas side effects and toxicity can be decreased.

Chemical analysis of a variety of different samples is involved in all areas of pharmaceutical research. Miniaturization of the analytical techniques results in fast and simple analysis of small sample volumes with reduced costs. Simple and portable miniaturized analytical devices have also enabled point-of-care analysis in e.g., doctor's office. These techniques could provide valuable tools also for precision medicine and screening of the individual characteristics. However, the robustness, precision, and sensitivity of the microfluidic analytical devices should be further addressed before these techniques can compete with conventional methods in pharmaceutical research. The aim of this thesis was to evaluate the feasibility of microfluidic analytical techniques for pharmaceutical research. A particular emphasis was put on drug metabolism and its impacts on precision medicine.

In the first subproject of this thesis, the effect of nanoformulations on CYP metabolism were determined in vitro. Three types of porous silicon (PSi) nanoparticles and three polymers commonly used in the same nanoformulations were investigated. Statistically significant alterations were observed in activities of the studied isoenzymes in the presence of the PSi nanoparticles, whereas polymers had less effect on the enzyme kinetic parameters. The highly polymorphic CYP2D6 was found to be most prone to inhibition by both the nanoparticles and the polymers. The results demonstrate the risk of interactions caused by other components of the (nano)formulations than the active ingredients. The effects of nanocarriers on CYP metabolism should be further investigated both in vitro and in vivo, to be able to evaluate the overall effects on CYP metabolism.

In the second subproject, a paper microfluidic assay was developed for rapid screening of the inter-individual differences in CYP enzyme activities. The multiplexed microfluidic lateral flow assay was based on a paper-like functionalized calcium carbonate coating and inkjet printed hydrophobic fluid barriers. The assay was applied to study of individual differences in CYP2A6 and CYP1A2 activities in (human) liver microsomes (HLM) of individual donors. The determined CYP activities were compared to average activities in a 20-donor subpopulation. The results showed both increased and decreased enzyme activities in the HLM of individual donors compared to the pooled HLM. However, based on the comparison to in-solution assays, further validation of the microfluidic lateral flow assay is needed to reach the robustness and sensitivity required for routine use.

In the third subproject, a commercial microchip electrophoresis (MCE) device with integrated electrochemical (EC) detection was applied to CYP metabolism studies and to analysis of morphine in mouse plasma and brain samples. The method developed for analysis of CYP metabolites showed good selectivity and precision. However, the sensitivity of the MCE-EC method was found insufficient for CYP metabolism studies. Instead, MCE-EC was shown to be feasible for quantitation of intraperitoneally administered morphine in mouse plasma and brain. Quantitation of morphine from biological samples was achieved with good precision and accuracy after off-chip liquid-liquid extraction (LLE) and on-chip electrokinetic stacking demonstrating the capability of MCE in targeted quantitative analysis.

In the fourth subproject, MCE was combined with electrospray ionization-mass spectrometry (ESI-MS). The method was applied to separation of phosphorylated peptides, particularly the positional phosphorylation isomers, which is a challenging task for conventional analytical techniques. The feasibility of the method was demonstrated with the help of monophosphorylated and triply phosphorylated insulin receptor peptides, which could be separated from the nonphosphorylated peptide in less than 40 s. The separation of the monophosphorylated peptide isomers from each other was achieved after derivatization.

In conclusion, with help of selected applications, this thesis demonstrates the advances that microfluidics could provide for conventional pharmaceutical analysis and drug metabolism studies. MCE was shown to be suitable for quantitative analysis with good precision and selectivity. Sensitivity is a common challenge in the field of microfluidics, but with carefully selected method for each application, these techniques can reach the benefits of miniaturized analytical devices. Further improvements in integration of the sample pretreatment and enrichment on the same microchip would also enhance the sensitivity as well as decrease the variation associated with manual sample handling.

PREFACE

This work was carried out at the Division of Pharmaceutical Chemistry and Technology, Faculty of Pharmacy, University of Helsinki, during the years 2013–2019. Doctoral Programme in Drug Research, Doctoral School in Health Sciences, and the European Research Council are acknowledged for funding this work.

First of all, I want to thank my supervisors Docent Tiina Sikanen, Professor Risto Kostiainen, and Professor Tapio Kotiaho. I am grateful to Tiina for the opportunity to work in the Chemical Microsystems group and for all her support and guidance during these years. I highly appreciate her dedication to science. I am also grateful to Risto and Tapio for their valuable advice and comments.

I want to thank all the collaborators and co-authors of the publications included in this thesis: Ashkan Bonabi and Doctor Ville Jokinen for the fabrication of numerous chips, Ermei Mäkilä, Dr. Dongfei Liu, Associate Professor Hélder Santos, and Professor Jarno Salonen for providing the nanoparticles, Docent Teemu Aitta-aho for the mouse samples, Eveliina Jutila, Risto Koivunen, Dr. Roger Bollström, and Professor Patrick Gane for providing the microfluidic lateral flow assays, and Michaela Koburg, Tea Pihlaja, Markus Haapala, Nina Nordman, and Arttu Kallio for their help in the laboratory. Professor James P. Landers and Docent Ari Tolonen are acknowledged for reviewing of this thesis.

Warm thanks go to the present and former members of the Division of Pharmaceutical Chemistry and Technology. The atmosphere in the lab, in the office, as well as in the coffee room brightens up each day at work. Many of you have become very close friends for me during these years.

Finally, I want to thank my family and friends for their support. My parents have always believed in me and helped me in every possible way. My friends especially in the choir Wiipurilaisen Osakunnan Laulajat and in the “dog world” have also been very supportive and encouraging, but with them I can also have a break from the work and focus on something completely different.

Helsinki, September 2019

Elisa Ollikainen

CONTENTS

LIST OF ORIGINAL PUBLICATIONS

This thesis is based on the following publications:

I Ollikainen E., Liu D., Kallio A., Mäkilä E., Zhang H., Salonen J., Almeida Santos H., Sikanen T.: The Impact of Porous Silicon Nanoparticles on Human Cytochrome P450 Metabolism. Eur J Pharm Sci (104), 124–132, 2017

II Ollikainen E., Koivunen R., Jutila E., Haapala M., Pihlaja T., Bollström R., Gane P., Sikanen T.: Paper microfluidics for precision medicine: Prediction of Patient Response to Drug Therapy with a Lateral Flow Cytochrome P450 Activity Assay (manuscript).

III Ollikainen E., Aitta-aho T., Koburg M., Kostiainen R., Sikanen T.: Rapid analysis of intraperitoneally administered morphine in mouse plasma and brain by microchip electrophoresis-electrochemical detection. Sci Rep (9), 3311 (9 pp), 2019

IV Ollikainen E., Bonabi A., Nordman N., Jokinen V., Kotiaho T., Kostiainen R., Sikanen T.: Rapid Separation of Phosphopeptides by Microchip Electrophoresis-Electrospray Ionization Mass Spectrometry. J Chromatogr A (1440), 249–254, 2016

The publications are referred to in the text by their Roman numerals.

Author's contribution to the publications included in this thesis:

I The experimental work, excluding nanoparticle preparation and characterization, was carried out by the author with some contribution from Arttu Kallio. The manuscript was written by the author with contributions from the coauthors.

II The experimental work was carried out by the author, excluding the preparation of the paper-based devices, which was done by Eveliina Jutila and Risto Koivunen. The manuscript was written by the author and Tiina Sikanen with contributions from the other coauthors.

III The experimental work was carried out by Michaela Koburg under the supervision of the author. Planning of the experiments and data handling was done by the author. The mouse samples were provided by Teemu Aitta-aho. The manuscript was written by the author with contributions from the coauthors.

IV The experimental work was carried out by the author excluding the microfabrication, which was done by Ashkan Bonabi. The manuscript was written by the author with contributions from the coauthors.

ABBREVIATIONS

7-HFC	7-hydroxy-4-trifluoromethylcoumarin
7-MFC	7-methoxy-4-trifluoromethylcoumarin
ACN	acetonitrile
AE	auxiliary electrode
AKD	alkyne ketene dimer
Alkyne-THCPSi	alkyne-terminated thermally hydrocarbonized porous silicon
AMHC	3-[2-(*N*,*N*-diethyl-*N*-methylammonium)ethyl]-7-hydroxy-4-methylcoumarin
AMMC	3-[2-(*N*,*N*-diethyl-*N*-methylammonium)ethyl]-7-methoxy-4-methylcoumarin
APTES-TCPSi	aminopropylsilane-modified thermally carbonized porous silicon
BGE	background electrolyte
CE	capillary (zone) electrophoresis
CEC	3-cyano-7-ethoxycoumarin
CHC	3-cyanoumbelliferone (3-cyano-7-hydroxycoumarin)
chipLC	microchip liquid chromatography
CL_{int}	intrinsic clearance
CV	coefficient of variation
CYP	cytochrome P450 (enzyme)
EC	electrochemical detection
EGE	ethylene glycol ether
ePAD	electrochemical paper-based analytical device
ESI	electrospray ionization
ex/em	excitation/emission (wavelengths)
FCC	functionalized calcium carbonate
FDA	the United States (U.S.) Food and Drug Administration
Fmoc-Cl	9-fluorenylmethyl chloroformate
Fmoc-OSu	9-fluorenylmethyl *N*-succinimidyl carbonate
HLM	human liver microsome
ICH	the International Conference on Harmonisation of Technical Requirements for Pharmaceuticals for Human Use
IR0	nonphosphorylated insulin receptor peptide
IR1A/B	monophosphorylated insulin receptor peptide (isomers A and B)
IR3	triply phosphorylated insulin receptor peptide
K_m	Michaelis constant
LC	liquid chromatography
L_{eff}	effective separation length
LIF	laser-induced fluorescence
LLE	liquid-liquid extraction

LOD	limit of detection
(L)LOQ	(lower) limit of quantitation
MCE	microchip capillary electrophoresis
ME	methyl ether
MES	2-(*N*-morpholino)-ethanesulfonic acid
MS	mass spectrometry
MS/MS	tandem mass spectrometry
μPAD	microfluidic paper-based analytical device
μTAS	miniaturized total (chemical) analysis system
NADPH	β-nicotinamide adenine dinucleotide 2'-phosphate
PDMS	polydimethyl siloxane
PSi	porous silicon
PVA	polyvinyl alcohol
Q-TOF	quadrupole-time of flight (mass spectrometer)
RE	reference electrode
R_f	retention factor
TCPSi	thermally carbonized porous silicon
UPLC	ultrahigh pressure liquid chromatography
UV	ultraviolet
V_{max}	maximal enzyme activity
WE	working electrode

1 INTRODUCTION

Chemical analysis of a sample consists of multiple steps including sample pretreatment, injection/introduction of the sample to the analytical system, separation, and detection of the analytes. The concept of a miniaturized total (chemical) analysis system (μTAS), combining all these steps on a single device, was first introduced almost 30 years ago.[1] By reducing the size of the analytical system, the sample and solvent consumption is decreased and the analysis times are shorter compared to conventional analytical systems, which commonly results also in reduced costs. Small size combined with integration of all analytical steps open up possibilities for portable devices and parallelization.

In drug discovery and development, the possibility for fast screening of e.g., metabolic properties could enhance the process and decrease the costs significantly. The conventional analytical systems are often too slow for screening of large amount of new drug candidates in the early phases of the development process. However, early identification of properties not preferable for a drug compound and termination of the development process will decrease the time and money spent in the later, more expensive development phases. Metabolic profile of the new drug candidate, including also the inhibitory and inductive effects, is one of these important properties that should be investigated in early phase of the development.

Drug metabolism refers to the enzymatic reactions taking place in the human body after administration of the drug. These reactions modify the drug so that it is more easily excreted. Metabolism can be divided in to two phases based on the reaction types: phase I reactions are mainly oxidation and reduction reactions that result in new functional groups that can then be conjugated in phase II reactions. The phase I reactions are catalyzed mainly by cytochrome P450 (CYP) enzymes, and a majority (70–80%) of drugs in clinical use as well as many other xenobiotics are metabolized by these enzymes.[2,3] Miniaturized analytical systems could provide simple and fast methods for screening of the metabolic properties of new drug candidates in reasonable time.

Miniaturized analytical devices are also commonly applied to point-of-care diagnostic systems.[4] These systems are ideally simple, fast, and low-cost devices that enable immediate result without additional laboratory equipment or trained personnel, e.g. in the doctor's office. Traditionally, the doctor prescribes a medication for a patient based on the diagnose. Current research has, however, been directed more towards tailoring of the treatment based on individual characteristics (including metabolic activity) instead of "one-size-fits-all" type of medication. The idea of this emerging approach called *precision medicine*, is to recognize the individual characteristics affecting to the treatment, and to select the most effective and safe medication for each

patient. The U.S. National Research Council recommends the term *precision medicine* to be used instead of the term *personalized medicine*, as the latter can be misinterpreted to refer to development of unique medications.[5] The adoption of precision medicine principles for widespread use requires fast and simple techniques for screening of the individual characteristics e.g., by miniaturized analytical techniques. Targeted drug delivery, with the help of nanocarriers, is another precision medicine approach.[6] The controlled release of the drug from the nanoformulation at the targeted site increases the bioavailability and efficacy, but also decreases the adverse effects and toxicity.

In this thesis, different miniaturized analytical systems were evaluated targeting selected analytical challenges in pharmaceutical research, drug metabolism, and the individual differences in CYP enzyme activities. Pharmaceutical nanoformulations, based on porous silicon (PSi) nanoparticles, were examined in terms of their effects on drug metabolism (I). In publication II, a simple microfluidic paper-based platform was developed and characterized for screening of individual differences in CYP enzyme activities. The feasibility of microchip electrophoresis (MCE) was investigated in three different applications. A simple, commercial device with integrated amperometric detection was used for CYP metabolism studies and for quantitative analysis of a targeted analyte in biological samples (III). A customized MCE system combined to mass spectrometry was applied for separation of phosphopeptides, including phosphorylation isomers (IV).

1.1 ROLE OF DRUG METABOLISM IN EFFICACY AND SAFETY OF THE TREATMENT

Identification of the efficacy and safety of a new drug candidate is a key point in drug discovery and development. Appropriate balance of safety and efficacy depends on the indication (severity of the condition, other available medications) and it can be evaluated by calculating the therapeutic index.[7] Traditionally therapeutic index is calculated as the ratio of the highest dose without toxic effects to the dose with the desired effect. Also exposure to the drug can be used instead of the actual dose as it considers also the variation between individuals, whereas same dose can result in different exposure levels. There is no universal limit of acceptable therapeutic index, but generally higher value describes more preferable safety profile. Instead, low therapeutic index may be acceptable for treatment of life-threatening diseases, especially if other options for treatment do not exist.

Drug metabolism has a major role in the efficacy and safety of the medication through the pharmacokinetic properties. Thus, drug metabolism research is one of the key points in drug discovery and development.[8] Fast metabolism, especially before the drug even reaches systemic blood circulation (first-pass metabolism), leads to low bioavailability for orally administered drugs. The metabolism of a new drug candidate should be well characterized

also to identify the functional groups most prone to metabolism (soft spots). The properties of the compound can then be further modified by blocking these soft spots. An ideal drug compound, from metabolism perspective, would not affect the activity of drug-metabolizing enzymes, and it would be metabolized by multiple enzymes, instead of only one.[8] These issues are further discussed in the following chapters. If reactive metabolites are formed, they may in turn react rapidly with e.g., cellular proteins or DNA, resulting in toxic effects [8,9] and thus, these are usually avoided.

CYP enzymes are the main drug metabolizing enzymes and they exist in all tissues, while they are most abundant in liver and small intestine.[10] These membrane-bound hemoproteins are mainly located in the endoplasmic reticulum of the cells.[11] Currently 18 families and 44 subfamilies of CYPs are known, but the enzymes metabolizing xenobiotics (including drugs) belong to families 1–3.[10] The other CYP enzymes participate in endogenous functions like biosynthesis of steroids and cholesterol, vitamin metabolism, and oxidation of unsaturated fatty acids. The CYP isoforms participating in drug metabolism and the fraction of drug compounds metabolized by each of them are presented in Figure 1.

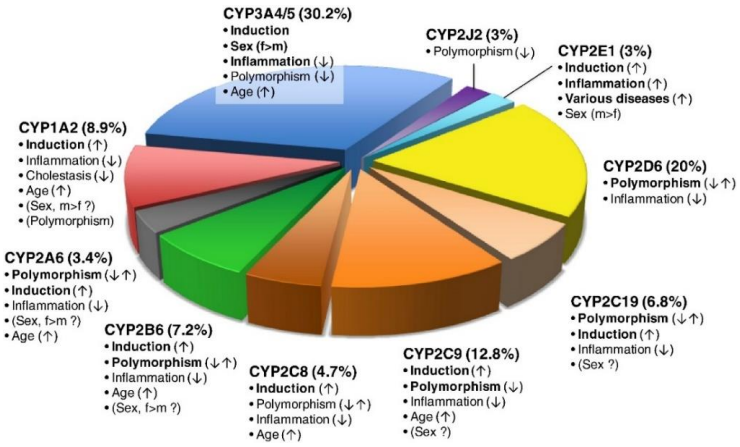

Figure 1 Factors affecting the cytochrome P450 activity and the fraction of clinically relevant drugs metabolized by the different isoforms (based on analysis of 248 drug metabolism pathways). Only the major contributing isoform is included for each metabolic pathway. The most important factors affecting enzyme activity are bolded and the arrows indicate the direction of the change (↑: increased activity; ↓: decreased activity). The effect of factors listed in parenthesis is controversial. Reproduced from ref. [3] originally published in Pharmacology and Therapeutics licensed under CC BY-NC-ND 4.0 (https://creativecommons.org/licenses/by-nc-nd/4.0/).

1.1.1 INDIVIDUAL CHARACTERISTICS AFFECTING DRUG METABOLISM

The activity of the CYP enzymes varies a lot between individuals and can lead to unexpected consequences in terms of safety and efficacy, if not carefully considered.[3] Generally, decreased enzyme activity results in high and even toxic concentration levels, whereas increased activity causes unintentionally low concentrations and lack of efficacy. The factors affecting CYP activity include genetic differences, other individual factors (age, sex), as well as inhibition or induction by drugs or other xenobiotics. The importance of these factors differs also between the different isoenzymes: for example, CYP2D6 is mainly affected by polymorphism and has been generally considered noninducible [3], even though some studies showing possible induction have also been published.[12] Instead, CYP3A4 is induced by a wide variety of substances and is also strongly affected by sex. The factors affecting enzyme activity, with examples of their clinical impact, are discussed in the following chapters.

Genetic polymorphism of cytochrome P450 enzymes

Polymorphism of CYP enzymes causes notable inter-individual and inter-ethnic differences in enzyme activities and thus alterations in efficacy, safety, and adverse effects of drugs. It has been estimated that out of all drug therapies, 20–25% result in unexpected outcome due to polymorphism mainly related to CYP enzymes.[13,14] To avoid these risks related to polymorphism, a new drug candidate should preferably be metabolized by multiple enzymes rather than just a single one [8], as mentioned previously.

The variations in *CYP* genes include single nucleotide polymorphism (substitution, insertion, or deletion of a single nucleotide) and copy number variation (gene duplication or deletion).[10,14] The enzymes most affected by polymorphism are CYP2D6, CYP2C19, CYP2C9, CYP2B6, CYP3A5, and CYP2A6.[3] People can be divided in to ultrarapid metabolizers, extensive metabolizers, intermediate metabolizers, and poor metabolizers.[3,10,14] The ultrarapid metabolizers have more than two active genes encoding a single CYP enzyme and they typically suffer from poor efficacy of drug therapies due to rapid elimination of the active drug. Extensive metabolizers are the "normal" phenotype with two functional genes, and usually the majority of the population belongs to this group. Intermediate metabolizers can have either one functional and one defective allele, or two partially defective alleles. Poor metabolizers are completely lacking the functional enzyme either due to defective gene or due to deletion of the gene, which may expose them to adverse effects and toxic doses.

The different types of metabolizers are not equally localized across the world, but significant ethnic differences have been observed.[15] For example, increased activity of CYP2D6, due to gene duplication, is most common in certain African populations (up to 29%) [15] and it can cause ultrarapid

elimination of e.g., tricyclic antidepressants resulting in inefficient treatment.[16] The duplication of *CYP2D6* gene may also result in e.g., ultrarapid metabolism of opioid painkiller tramadol to its active metabolite, which can cause respiratory depression if the patient's renal function is also decreased.[17] In turn, polymorphism of CYP2D6 resulting in decreased enzyme function is observed with highest frequency in East Asian population (70.3%).[15] These poor metabolizers have higher risk for adverse effects of e.g., antipsychotic risperidone, which may end up in termination of the treatment.[18] Another example is the CYP2C9 deficiency, most commonly observed in Europeans, Africans and South Asians, which is at least partly involved in the wide inter-individual differences in doses of the anticoagulant warfarin, and the difficulty of some patients to reach the narrow therapeutic window.[15,19]. The typical initial doses of warfarin may cause high risk of bleeding if the patient is poor metabolizer but the dose is not adjusted accordingly. CYP2A6 deficiency is in turn most commonly observed in Japanese and Korean populations with frequencies of 50.5% and 42.9%, respectively, compared to only 9.1% in white populations.[20] This results in notable differences e.g., in the rate of nicotine metabolism catalyzed by CYP2A6.

Other individual characteristics affecting cytochrome P450 activity

In addition to polymorphic differences, other individual characteristics, including sex, age, and diseases, affect the activity of CYP enzymes (Figure 1).[2,3,10] Sex-related differences in CYP activities show higher activity of CYP2D6, CYP3A4 and CYP2A6 in females than males, whereas CYP1A and CYP2E1 are more active in males.[3,21–23]

The effect of age is observed as decrease in metabolism capacity during the first year of life and in old age.[3] The enzyme system is not fully developed in neonates, and instead of the CYP3A4 of adults, the most prominent enzyme of the CYP3A subfamily during fetal period is CYP3A7. In elderly people, decrease in enzyme activity or expression have not been observed (rather the opposite), even though the ability to metabolize drugs is clearly decreased.[3,22] This difference might be related to common use of multiple medications affecting the enzyme activities, and to decreased blood flow in liver.

CYP activities are also altered in many diseases, but the effects vary between the different CYP enzymes from decreased to increased activity.[24–26] In liver diseases the loss of functional hepatocytes is one of the mechanisms causing decreased activities of CYP enzymes, while other factors may also exists. CYP1A, CYP2C19, and CYP3A activities are generally most decreased [26], but the effects on different CYPs are also dependent on the etiology and severity of the liver disease. For example, in nonalcoholic fatty liver disease the expression and activity of CYP1A2, CYP2C19, CYP2D6, and CYP3A4 are decreased together with progress of the disease, whereas activities

of CYP2A6 and CYP2C9 are increased.[25] In addition to liver diseases, also infections, inflammations, and cancers typically decrease the expression of CYP enzymes.[3,27,28] Also, obesity results generally in decreased CYP activity, except CYP2C and CYP2E1 enzymes, that may show even increased activities.[29]

1.1.2 EXTERNAL FACTORS AFFECTING DRUG METABOLISM

Enzyme inhibition and induction by external chemicals also affect drug metabolism, occurrence of adverse effects, and efficacy of the medication due to decreased or increased enzyme activity. Today, if a new drug candidate is found to have a high risk of drug-drug interactions, the development is typically terminated.[8] Enzyme induction mechanisms are typically quite complex and there is lots of variability between different isoenzymes.[30] However, in most cases induction results from increased protein synthesis via ligand activation of key receptor transcription factors, e.g., pregnane X receptor (PXR), constitutive androstane receptor (CAR), or aryl hydrocarbon receptor (AhR).

Enzyme inhibition

Enzyme inhibitors are classified to irreversible and reversible inhibitors, and the latter are subdivided to competitive, noncompetitive, and uncompetitive inhibitors (Figure 2).[31] In reversible inhibition, the inhibitor usually binds to the enzyme easily, but not permanently. In competitive inhibition, the substrate and the inhibitor compete for binding to the same active site of the enzyme, whereas in noncompetitive inhibition the inhibitor binds to a different site and changes the conformation of the enzyme so that the substrate is unable to bind to the active site. Uncompetitive inhibition takes place only after formation of enzyme-substrate complex. Mixed-type inhibitors with properties of both competitive and noncompetitive inhibitors are also commonly observed. Irreversible inhibitor is typically metabolized by the CYP enzyme to form a reactive metabolite which binds covalently to the enzyme and causes permanent inactivation.[31,32] The activity recovers only after synthesis of new enzymes.

CYP enzymes can be inhibited by drugs, but also by other chemicals, e.g. pesticides, or by dietary substances. A well-known and widely investigated example of food-drug interaction is the irreversible inhibition of CYP3A enzymes by furanocoumarin derivatives in grapefruit juice.[33] Also, a common flavoring agent, menthol, is shown to inhibit CYP2A6 resulting in decreased nicotine metabolism.[34,35] Smoking of mentholated cigarettes slows down the metabolism of nicotine resulting in higher systematic nicotine exposure compared to smoking of nonmentholated cigarettes. Humans are also exposed to wide variety of other chemicals and the metabolic effects are

not always very well known. In human liver microsomes (HLM), organophosphate pesticides inhibit CYP1A1/2 and CYP2B6, whereas pyrethroid insecticides showed inhibitory potential towards CYP2D6 and CYP3A4.[36] Parabens and phthalates commonly used in e.g., cosmetics and plastics, may have inhibitory effect on CYP enzymes as well.[37] Also, alterations in CYP activity are linked to nanomedicines, including viral vectors and silver and gold nanoparticles [38], which are emerging tools for targeted drug delivery in precision medicine.[39]

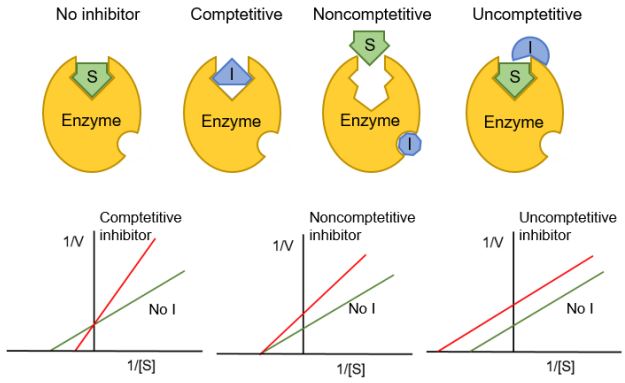

Figure 2 Up: A schematic presentation of the different reversible enzyme inhibition mechanisms. S: substrate; I: inhibitor. Down: The effects of different inhibitor types on Lineveawer-Burk graphs. Red line: with inhibitor; green line: no inhibitor.

1.1.3 SCREENING OF INDIVIDUAL DIFFERENCES IN ENZYME ACTIVITIES

Screening of individual CYP activities before prescribing a treatment for a patient would be beneficial, especially in case of multiple medications or drugs with very narrow therapeutic window. The U.S. Food and Drug Administration (FDA) has added recommendations of CYP genotype testing and adjusted dosage in a set of product labels, including the anticoagulant warfarin with narrow therapeutic window and high risk of severe adverse effects.[40,41] Also, in case of unexpected drug responses, investigation of the CYP activities could provide explanation and help in adjusting the medication.

Few different commercial tests for fast and simple determination of genetic polymorphism are available.[10,42] However, these are limited mainly to the most common variants of *CYP2D6*, *CYP2C9*, and *CYP2C19*, whereas rare variants will not be detected. Another disadvantage of these assays is that all the other sources of individual variation described in previous chapters are not considered. More complete information of the CYP activities can be obtained by administration of a probe drug that is metabolized by a single CYP enzyme. The ratio of the parent drug and its specific metabolite in urine, blood, or saliva is then monitored to determine the enzyme activities.[10,42] Administration

of the probe drugs in therapeutic doses may however result in adverse effects especially if multiple probes are used (cocktail assay) to investigate activity of more than just one CYP enzyme. In addition, these methods typically require frequent sampling for up to 8 hours, even though also new simple methods enabling single analysis of a dried blood spot are developed to facilitate the analysis of metabolic ratio.[43] In the future, individual alterations in CYP activities will most likely be considered also in terms of precision medicine.

1.2 MICROFLUIDIC ANALYTICAL SYSTEMS

The first miniaturized separation device, a gas chromatograph, was developed more than 10 years before the introduction of the μTAS concept [44], but the real interest in microfluidic separation systems was not increased until 1990's. Since then, many analytical separation techniques have been miniaturized to increase the throughput by faster analysis, integration of multiple operations, and parallelization. In addition, miniaturization results in decreased sample and solvent consumption and reduced costs. In the following chapters, miniaturization of capillary (zone) electrophoresis (CE) and liquid chromatography (LC) are prescribed, as these techniques are typically most suitable for analysis of (small molecule) pharmaceuticals. In addition, feasibility of microfluidic paper-based lateral flow assays for pharmaceutical applications are discussed.

1.2.1 MICROCHIP ELECTROPHORESIS

In conventional CE, the sample is injected to a capillary filled with electrolyte solution and an electric field is applied across the capillary to create electroosmotic flow towards the detector in the other end of the capillary. The charged analytes are separated in the capillary based on their different electrophoretic mobilities (size and charge of the molecule). CE is a relatively simple technique and inherently suitable for miniaturization, and thus microchip electrophoresis (MCE) has become the most commonly miniaturized separation technique.[45] Also other electromigration techniques, including isoelectric focusing [46,47], isotacophoresis [48], micellar electrokinetic chromatography [49,50], electrochromatography [51], and gel electrophoresis [52,53], have been miniaturized. In this thesis, only miniaturization of capillary (zone) electrophoresis is discussed, as it is the most widely applied electromigration technique in analysis of pharmaceuticals and related small molecules.

The separation principle of MCE is the same as in conventional CE, but in MCE the separation takes place in a microfabricated channel (few centimeters long, typically rectangular cross-section) instead of a round capillary (ca. 1 m long). A great benefit of MCE over conventional CE is the easy manipulation of very small volumes of fluids and especially the possibility to inject a very

narrow sample plug defined by the intersection of the microfabricated channels (Figure 3).[45,54] The narrow initial sample plug enables the use of short separation channels in MCE and thus much faster separation of the analytes compared to conventional CE. The sample can be injected electrokinetically from an injection channel to the separation channel resulting in reproducible injection in picoliter scale. The most common channel geometries include simple cross and offset (double-T) designs (Figure 3), where the sample flows across the separation channel as a result of electric field applied across the injection channel.[54] When the electric field is switched across the separation channel, the sample plug defined by the geometry of the injection cross, is introduced to the separation channel (floating injection, Figure 3).[55] The repeatability of the injection can be further increased by preventing sample leakage to the separation channel during the injection step by applying small focusing potential to buffer inlet and outlet (pinched injection, Figure 3). Similarly, small push-back voltages can be applied to the sample inlet and sample waste during the separation step to "push" the rest of the sample back to the injection channel.

The first MCE devices were fabricated of glass by micromachining techniques adopted from semiconductor industry.[45,56,57] Glass has beneficial properties including optical transparency and thermal stability. In addition, it is very hard material and the surface can be easily modified based on the silane chemistry, but fabrication of glass devices requires cleanroom facilities and is relatively complex and expensive.

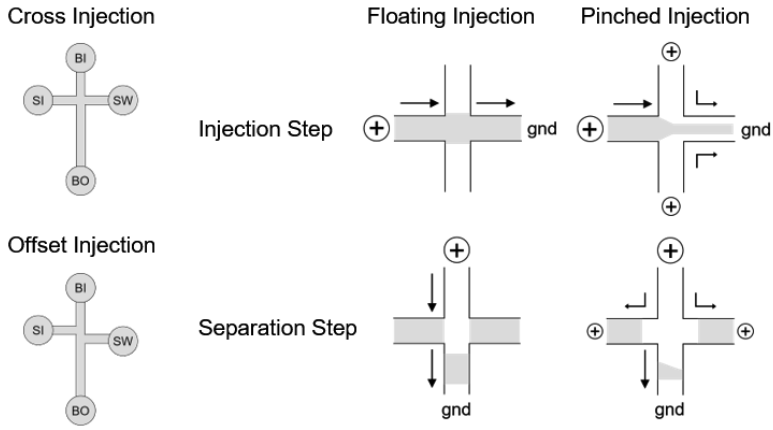

Figure 3 Schematic view of typical MCE channel designs (left) and of applied voltages in floating and pinched injection modes during injection and separation steps (right). The arrows show the direction of the liquid flow. BI: buffer inlet; BO: buffer outlet; SI: sample inlet; SW: sample waste; gnd: ground. Injection channel from SI to SW, separation channel from BI to BO. Grey: sample; white: background electrolyte.

Polymers have been investigated as alternative materials for microfluidic devices as they are generally cheaper and easier to fabricate, and thus better suitable for disposable devices.[56,58] In addition, a wide variety of polymers with different chemical, mechanical, and optical properties exist, which enables selection of the most suitable material for each application. The first polymer-based MCE device was fabricated of the elastomer polydimethylsiloxane (PDMS).[59] Currently, PDMS is the most commonly used microfabrication material in microfluidic research since it is inherently biocompatible and suitable for fast prototyping outside cleanroom conditions.[56] However, the hydrophobic surface is prone to nonspecific adsorption of analytes and thus surface modifications are needed before PDMS devices can be used for analytical purposes. Despite the wide use of PDMS in academic world, it is typically avoided in commercial devices as it is not very well suitable for large-scale fabrication.[56] Many other polymers are also investigated, including e.g., poly(methylmethacrylate) (PMMA) [60], polycarbonate [61], epoxy photoresist SU-8 [62], and thiol-enes [63,64], to overcome some of the limitations related to PDMS. The most important properties of the materials regarding MCE include inert surface chemistry to avoid nonspecific interactions and to maintain EOF. Depending on the detection method, also optical transmittance and clarity are often desired.

Detection methods

In conventional separation systems, the most common detection methods for analysis of pharmaceuticals and related small molecules are ultraviolet (UV) absorbance, mass spectrometry (MS), fluorescence, and electrochemical (EC) detection. The first MCE systems were combined with laser induced fluorescence (LIF) as a detection method.[55,65–67] It is a sensitive method due to low background noise (especially on glass chips) and it is relatively easy to combine with the MCE system. Today, it is still very commonly used even though the detection itself is generally not miniaturized but requires bulky instrumentation e.g., microscopes, excitation sources, and photomultiplier tubes.[45,68] Few studies on miniaturization of fluorescence detection have been performed utilizing light emitting diodes (LED) as excitation source.[69–71] The miniaturized detection system was combined with MCE and applied for analysis of endogenous biomarkers and pharmaceuticals from urine and plasma samples. However, the analytes required off-chip fluorescence labeling, which inevitably increases the analysis time and the manual work load. Most pharmaceuticals and related small molecules are not inherently fluorescent and require derivatization, which may complicate the process unless the fluorescence labeling is integrated on the same microchip.

UV absorbance is widely used detection method in conventional bioanalytical systems, but in miniaturized systems the optical path length is typically very short, which decreases the sensitivity of absorbance detection significantly and thus its suitability for miniaturization.[72] Few devices with

e.g., integrated waveguides [73] or microlenses and detection cells with extended path length [74] exist for absorbance detection, but their use is limited to applications where high sensitivity is not required.[75]

EC has been combined with MCE for almost as long as LIF [45], amperometric detection being the most commonly miniaturized and best suited electrochemical method for bioanalytical applications.[76] Amperometric detection is based on reduction and oxidation (redox) reactions of the analytes at the working electrode (WE) surface.[77] A constant potential is applied to the WE and the redox reactions are observed as changes in the current, which is proportional to the analyte concentration. Detection sensitivity of EC is not decreased by miniaturization, but the signal-to-noise ratio can even be improved as the surface-to-volume ratio (of the WE and sample) is typically higher in miniaturized systems.[77,78] Fabrication of the electrodes is relatively easy with common microfabrication techniques and the electrodes can be directly integrated to the microchip, which simplifies the operation of the device. EC is also more universal detection method than fluorescence, and the selectivity of the detection can be further adjusted by the choice of the electrode material.[77] Pharmaceuticals do often have easily oxidized functional groups enabling easy EC detection. In addition, EC detection does not require large additional instrumentation (like LIF) and portability is easily achieved.[77,78]

In conventional bioanalysis mass spectrometry is a major detection method due to its high specificity, low detection limits, and quantitativity. Especially electrospray ionization (ESI) benefits from miniaturization.[79] The low flow rates in MCE enhances the production of smaller droplets, which in turn results in more efficient ionization and improved sensitivity. In addition, a sharp tip or nozzle is required to produce the spray. In the first miniaturized devices the spray was produced directly from a channel opening in the planar edge of the microchip.[80,81] The lack of sharp tip causes the sample to spread on the planar edge and high voltages were required to produce the spray. To overcome these challenges external nanospray emitters, e.g. silica capillaries or nanospray needles, were attached to the channel outlet to create a sharp nozzle.[82,83] However, the addition of external emitters increases manual work as well as dead volumes in the liquid junctions leading to peak broadening. Later, monolithically integrated sharp tips have been developed to avoid these issues.[84,85] The miniaturized ionization techniques are still mainly used with conventional, large, and expensive mass spectrometers, even though miniaturization of the entire instrument has also been investigated.[86] However, vacuum is required for efficient mass analysis, but if the vacuum pumps are miniaturized, their capacity will also be decreased, which is a limitation in developing completely miniaturized mass spectrometers.

Applications in pharmaceutical analysis

A wide range of MCE bioapplications have been published covering analysis of cells, cell components and lysates, DNA, proteins and peptides, and antibodies and antigens.[87] The applications in analysis of pharmaceuticals and related small molecules include analysis of pure drug compounds, active ingredients in pharmaceutical dosage forms, as well as drugs and/or their metabolites in biological matrices. Some applications in analysis of pharmaceuticals and related small molecules are listed in Table 1 sorted by the detection method. Generally, the reported limits of detection (LOD) and quantitation (LOQ) were in low micromolar level, but with mass spectrometric detection LODs from few nanomoles to tens of nanomoles per liter were achieved. The precision values of the MCE methods were also good, below 5% CV (coefficient of variation) in most cases. However, the concentrations used for determination of precision were often quite high and precision near LOD/LOQ was not generally reported.

Despite the almost 30 years of MCE analysis and variety of published applications, the method has not reached an interest comparable to e.g., conventional LC. One of the biggest questions is the robustness of the method and only few validated quantitative methods exists. MCE may not be able to compete in sensitivity with conventional methods in the most challenging applications, but not all applications require extreme sensitivity and there MCE could be most useful. The limits of detection (LOD) and precision are determined in many applications, but further validation according to the guidelines of e.g., the FDA [88] or the ICH (International Conference on Harmonisation of Technical Requirements for Registration of Pharmaceuticals for Human Use) [89] is not commonly completed. As an example of further validation, a quantitative MCE method with fluorescence detection for analysis of diuretics both in tablets and in urine samples was developed. [90] The method was validated in terms of linearity, limits of detection (LOD) and quantitation (LOQ), precision of peak area and migration time and recovery (from tablets). LOQs of 2 μg/mL or below were achieved with intraday precisions below 2.30% (CV).

Another challenge is the sample preparation. Many miniaturized on-chip sample preparation methods have been developed including e.g. solid-phase extraction [91–95], liquid-phase microextraction [96,97], and electromembrane extraction [98,99]. However, most of the MCE methods and applications still rely on off-chip (manual) sample preparation before the separation on chip with few exceptions of on-chip sample processing. An integrated labeling protocol was demonstrated in quantitative analysis of four thiol drugs with chemiluminescence detection, but the analysis of the drugs in plasma samples still required additional off-chip sample clean-up.[100] Also, an on-chip liquid-phase microextraction utilizing a porous membrane has been demonstrated in analysis of two painkillers, tramadol and paracetamol, and their metabolites in urine samples.[96]

Table 1. *Applications of MCE in pharmaceutical analysis.*

Analytes	Matrix	Sample prep.	Chip material[a]	LOD / LOQ	Precision[b]	Ref.
Electrochemical detection						
Dopamine, levodopa, epinephrine			*glass*	2.4–12.2 µM	1.6–1.9% (100–500 µM)	[101]
Dopamine, catechol			glass/PDMS	1.2 µM	2.8–3.9% (not reported)	[102]
Morphine, codeine	urine	off-chip SPE	PDMS	0.2–1 µM	4.2–5.7% (200 µM)	[103]
Uric acid, epinephrine, paracetamol	urine	off-chip	*glass/SU-8*	4–10 / 5-20 µM	2–4% (50–125 µM)	[104]
Caffeine, theophylline	serum, urine	off-chip SPE	PDMS	4 µM	3.8–4.9% (200 µM)	[105]
Mass spectrometric detection						
Tramadol, propranolol, bufuralol, verapamil		**on-chip SPE**	SU-8		11.5% (20 µM)	[91]
1'-Hydroxybufuralol		**on-chip LPME**	SU-8	9.3 / 31.2 nM	10.3% (80 nM)	[96]
Tramadol, paracetamol and their metabolites	urine	**on-chip LPME**	SU-8	4 nM		[96]
Propranolol	urine		*glass*[c]	2.2 nM		[106]
Fluorescence detection						
Penicillamine enantiomers		off-chip labeling	glass	0.5–1.1 µM	1.3% (20 µM)	[69]
Methamphetamine, ephedrines	pharmaceuticals, samples from clandestine labs	off-chip	*glass*			[107]
Sulfonamides	rabbit plasma, pharmaceuticals	off-chip labeling	glass	0.36–0.50 µg/mL	1.21–1.48% (12.5 µg/mL)	[71]
Amphetamine-type stimulants	tablets	off-chip labeling	*glass*		1.6–5.5% (not known)	[108]
Opioids, psychopharmaceuticals		**on-chip LPME**	*glass*		19–28% (10 µg/mL)	[97]
Serotonin, tryptophan, propranolol			silicon/glass	2–4µM		[73]

[a] commercial microchips are marked with italics

[b] coefficient of variation (CV), the concentration used for determination of precision is in parenthesis

[c] a pulled nanoelectrospray emitter was prepared to a commercially available glass chip

1.2.2 MICROCHIP LIQUID CHROMATOGRAPHY

Liquid chromatography (LC) is the most commonly used conventional separation technique in bioanalysis. The sample is injected to a liquid (mobile phase) which is pumped (pressure-driven flow) through a column packed with stationary phase. The analytes are separated based on their different interactions (retention) with the stationary phase. LC is suitable for analysis of a large variety of compounds as the methods can be adjusted by selecting appropriate stationary phase and mobile phase composition.

Microchip LC (from now on chipLC) is especially advantageous in applications with limited sample volume, where the miniaturization reduces dilution of the sample in the column and thus results in enhanced sensitivity.[109] ChipLC also enables development of portable instrumentation for e.g., on-site analysis or point-of-care diagnostics, and reduces solvent consumption and analysis time. However, implementation of LC on a microchip has not gained as much attention as MCE.

The main challenge in chipLC is the channel structure. In MCE a simple microchannel is needed for separation, which is relatively easy to fabricate. Instead, chipLC requires a more complex structure, as the stationary phase needs to be integrated in the channel. It can be integrated manually by adding small particles and frits to the channel [110], by adding a monolithic structure [111,112], or by fabricating microstructures, e.g. pillars [113,114], simultaneously with the channel.[115]

Another significant difference is the liquid handling as chipLC utilizes pressure-driven flow instead of electrokinetic flow. In chipLC a very precise and stable liquid flow with flow rates between nanoliters per minute to few microliters per minute is required while the operating pressures are around 700 bars or even higher.[115] Electroosmotic flow can, however, be utilized to create pressure-driven flow in non-mechanical pumps.[116–118] These electroosmotic pumps are relatively easy to fabricate and integrate as on-chip pumps, because they don't include any moving parts.[115,116] Also, a continuous pulse-free flow can be created and the direction of the flow can easily be changed by switching the polarity of the electric field. Other non-mechanical pumps include electrochemical [119,120], electrohydrodynamic [121], and magnetohydrodynamic pumps [122,123]. However, currently most chipLC systems utilize external mechanical off-chip pumps connected to the actual microchip, commonly either reciprocating pumps or syringe pumps.[115] The challenge in these systems is the dead volumes in liquid junctions of the connecting capillaries between pumps and the actual microchip: as the total volume in the system decreases, the proportion of the dead volume increases correspondingly causing peak broadening.[115,124] The low interest in development of chipLC may also be at least partly related to the fact, that commercial LC systems with decreased column, sample, and detection volumes (capillary and nano LC) already have some of the benefits

of miniaturization, including smaller solvent consumption and enhanced sensitivity.[115,124,125] However, the relatively large dead volumes in liquid junctions are a challenge also in these systems.

The first chipLC devices were prepared of silicon, but as it is not optically transparent in UV or visible light, it was replaced by glass-based devices.[115] In chipLC the system needs to stand high pressures, which limits the use of some polymers, especially PDMS.[56] Thermoplastics, including PMMA, polystyrene, are transparent and more rigid materials and thus better suitable for chipLC. However, many polymers suffer from poor solvent compatibility, which limits their use in chipLC, as organic solvents are commonly used in mobile phases.[58] Cyclic-olefin copolymer is an example of a hard and transparent material, which is also more tolerant to organic solvents.[115]

Optical detection, EC detection and mass spectrometry are the most common detection methods also for chipLC.[115] Fluorescence detection is the main optical method, but as described also in case of MCE, inherent fluorescence is not very common phenomena. Commercial vendors have been especially interested in developing instrumentation for integration of chipLC and MS.[115,126–129] Similarly as in the case of MCE, the chipLC is typically integrated with conventional large scale mass spectrometers disabling portability or analysis in the field. The high sensitivity of MS, however, enables analysis of very small amounts of the analytes. For example, a chipLC-MS/MS method was able to detect a set of abused drugs and their metabolites in human hair samples with limits of detection between 0.1 and 0.75 pg/mg hair and limits of quantitation between 0.2 and 1.25 pg/mg hair.[130] In another application, antidepressant fluoxetine and its metabolite norfluoxetine were analyzed from only 20 µL of rat serum by a chipLC-MS/MS method with LODs of 0.18–0.67 ng/mL.[131] Most likely the chipLC could benefit the field of drug discovery by enabling fast analysis of small sample volumes in laboratory conditions instead of on-field or point-of-care analysis.

1.2.3 PAPER MICROFLUIDICS

The concept of microfluidic paper-based devices (µPADs) was introduced in 2007 [132] following the principles of paper chromatography and lateral flow diagnostic assays (e.g. pregnancy tests) that have existed far longer.[133,134] Medical diagnostics and point-of-care/in-field analysis have been the main application areas of µPADs due to their special properties enabling simple and fast analysis.[135,136] A lot of applications of these disposable low-cost devices have been investigated for the needs of developing countries or resource-limited areas, where other laboratory equipment may not be easily accessible. Also applications in environmental and food safety monitoring have gained lot of attention.[134,135]

µPADs are typically implemented on a cellulose substrate, which provides unique properties compared to traditional microfabricated devices described in the previous chapters.[135] Cellulose is abundant, inexpensive, lightweight,

and biodegradable, and as a hydrophilic porous material it enables fluid flow generated by capillary action without any external pumps or power supplies.

Another attractive aspect is the easy fabrication of these devices. Hydrophobic areas are created to form liquid barriers and to control the fluid flow on the μPAD. A variety of deposition techniques exist (Figure 4) [137] and wax printing (Figure 4G) with standard office printer is one of the most commonly adopted methods.[134,135] After printing, the wax is melted through the porous cellulose-based substrate to create the channel walls. The development of new hydrophobic agents (e.g. alkyl ketene dimer, AKD) has increased the use of inkjet printing (Figure 4I), which enable fast and low-cost deposition with relatively high throughput and reproducibility.[134] In addition, the design of the channel structure can be easily modified and the new version of the device can be printed on demand.

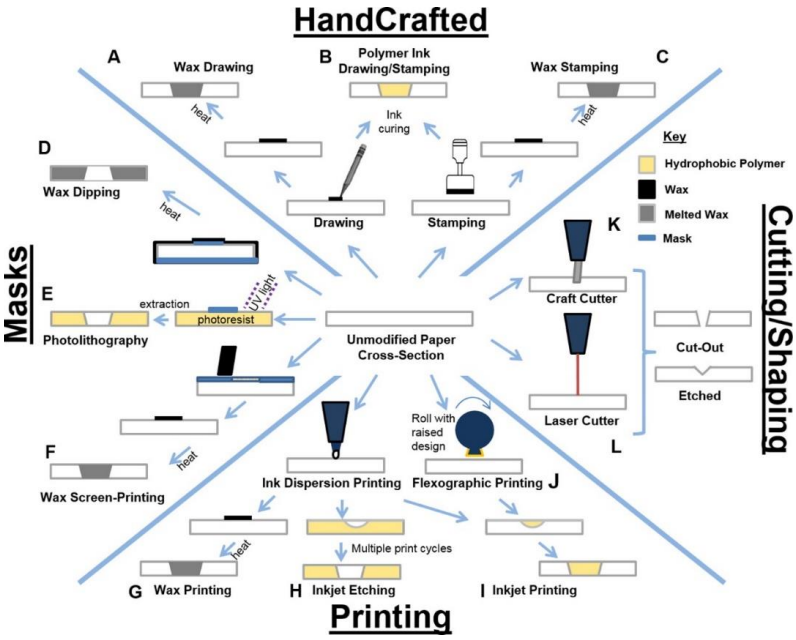

Figure 4 A schematic of different fabrication techniques of paper-based microfluidic devices. Hand crafted devices (top) can be fabricated by (A) wax drawing, (B) polymer ink drawing/stamping, or (C) wax stamping. Hydrophilic regions are protected with masks (left) in (D) wax dipping, (E) photolithography, and (F) wax screen-printing techniques. Printing techniques (bottom) include (G) wax printing, (H) inkjet etching, (I) inkjet printing, and (J) flexographic printing. For cutting and shaping air boundaries or etching channels, (K) a craft cutter or (L) a laser cutter can be used. Color codes: yellow: hydrophobic polymer; black: wax; grey: melted wax; blue: mask. Reprinted from ref. [134] with permission from ACS Journals.

Detection in μPADs is typically based on colorimetric methods.[134,135,138] It provides easy and simple readout without any additional instrumentation and is thus very easily suitable for point-of-care and in-field applications. Colorimetric methods are based on either simple yes/no answer or a set of multiple color reactions that are specific for a compound or a functional group in the structure. The latter approach can enable even identification of a compound. However, the sensitivity is not very good and for quantitative analysis, additional instrumentation is usually needed.[135] The worldwide distribution of smartphones has enabled a new approach, called "telemedicine".[139] Using a smartphone, a photo of the μPAD (after colorimetric reaction) can be send to a doctor or to a research laboratory for interpretation of the results. Also smartphone applications for result interpretation have been developed. EC detection can also be integrated to μPADs, in this case also called ePADs (electrochemical paper-based analytical devices), with relatively simple and low-cost methods.[140] The clear advantages of EC detection over colorimetric detection are the better sensitivity, selectivity, and quantitativity [135,140,141], while additional instrumentation is necessary.

In addition to the applications in medical diagnostics, only few spot-on tests for pharmaceutical applications have been developed. Screening of illegal drugs [142,143] and counterfeit or low quality pharmaceuticals [144–147] with a simple μPAD, has aroused interest, as no skilled personnel or laboratory equipment is needed. For example, a μPAD was developed for simultaneous detection and identification of multiple abused and illegal drugs, including opiates, phenethyl amines, cocaine, and ketamine (Figure 5, left).[142] The device consisted of 6 channels, with one or more colorimetric reagents in each. With combinations of the different reactions, each of the nine drugs could be detected and distinguished from each other based on the produced colors. Also semiquantitative analysis could be performed with smartphone and an image processing software. In another example, a quantitative colorimetric immunosorbent assay for analysis of ketamine in saliva was able to reach detection limit of 0.03 ng/mL. [143] However, the procedure included manual application of multiple reagents and additional heating and washing steps, decreasing the suitability for in-field analysis by non-experienced persons. In search of counterfeit or low quality pharmaceuticals, focus has been on β-lactam antibiotics [144,145] and antimalarial drugs [146,147], most likely due to their wide use in resource-limited areas. For example, a "β-lactam PAD" was developed for easy confirmation of the active ingredients in tablets.[144] The solid tablet was "swiped" across the device (Figure 5, right) and the PAD was then dipped in water to initiate the analysis. Based on a "color bar code" created from the 12 parallel lines with different reactants, the different β-lactam antibiotics could be identified. In addition, the μPAD was able to detect common excipients (e.g. starch) as well as "substitute" active ingredients that are typically used in falsified drugs.

Figure 5 Examples of µPADs based on colorimetric detection. Left: µPADs for detection of abused and illicit drugs. Top: analysis of blank sample; Bottom: analysis of morphine (positive result). Each channel is labelled with the abbreviation of the analytes detected and the color of the text shows the color produced in the case of positive result. Eph; ephedrine; MA: methamphetamine; MDMA: 3,4-methylenedioxide-methamphetamine (ecstasy); Coc: cocaine; Ket: ketamine; Cod: codeine; Theb: thebaine; Morph: morphine; Amp; amphetamine. Reproduced from ref. [142] with permission form Royal Society of Chemistry. Right: µPADs for screening of β-lactam antibiotics based on a color bar code. The studied tablet is "swiped" across the lines A-L. (a) 100% amoxicillin gives dark green in lane A, green in lane B, and orange in lane G. (b) A 2:1 w/w mixture of ampicillin and calcium carbonate gives blue-green in lane A, orange in lane B, and no color in lane G (indicating ampicillin rather than amoxicillin) and dark orange at the swipe line in lanes I and J (indicating carbonate). (c) Maize flour gives no API colors and dark purple at the swipe line in lane H (indicating starch). Adapted from ref [144] with permission from ACS Journals.

2 AIMS OF THE STUDY

The overall aim of the study was to evaluate the feasibility of microfluidic analytical methods for pharmaceutical research. Also, emphasis was put on drug metabolism research and precision medicine.

The microfluidic analytical techniques were evaluated in different types of pharmaceutical applications, including both quantitative and qualitative analysis by simple commercial devices as well as customized techniques. Sensitivity and robustness required for different applications were also evaluated. Drug metabolism was studied with a view to precision medicine by evaluating the effects of nanocarriers on CYP metabolism. One of the aims was also to develop a microfluidic method for screening of individual CYP activities as a tool for precision medicine.

The more detailed aims were

- to study the effects of porous silicon (PSi) nanoparticles and polymers commonly used in the same pharmaceutical nanoformulations on CYP enzyme activities and clearance
- to assess the need to examine the metabolic effects of nanocarriers as a part of toxicity and biocompatibility assessment
- to evaluate the suitability of a μPAD for screening of individual differences in metabolic activities of CYP enzymes
- to study the feasibility of a commercial MCE-EC device for quantitative analysis of targeted compounds in biological samples and for rapid analysis of CYP enzyme activities
- to assess the applicability of the above mentioned MCE-EC methodology for routine use in site of research, e.g. in animal laboratory
- to evaluate the power of MCE in challenging analytical tasks by developing an MCE-ESI/MS method for separation of phospho-peptides including separation phosphorylation isomers

3 EXPERIMENTAL

This section briefly describes the chemicals, materials, instruments and protocols used in the study. Details are provided in the original publications (I–IV).

3.1 CHEMICALS AND MATERIALS

Chemicals and materials used in this work are listed in Table 2. The notes indicate their use. The CYP probe substrates and corresponding metabolites are listed in Table 3.

Table 2. *Chemicals and materials used in the study.*

Chemical/Material	Manufacturer/Supplier	Note	Publication
2-(*N*-morpholino)-ethanesulfonic acid (MES) hydrate	Sigma-Aldrich, Steinheim, Germany	Reagent	II, III
2-Propanol	Sigma-Aldrich, Steinheim, Germany	Solvent	III
9-Fluorenylmethyl chloroformate (Fmoc-Cl)	Sigma-Aldrich, Steinheim, Germany	Derivatization reagent	IV
9-Fluorenylmethyl *N*-succinimidyl carbonate (Fmoc-OSu)	Sigma-Aldrich, Steinheim, Germany	Derivatization reagent	IV
Acetic acid	Sigma-Aldrich, Steinheim, Germany	Reagent	IV
Acetonitrile	Sigma-Aldrich, Steinheim, Germany	Solvent	I, II, IV
Ammonium acetate	Sigma-Aldrich, Steinheim, Germany	Reagent	IV
Ammonium sulfate	Riedel-de Haën, Seelze, Germany	Reagent	III
β-nicotinamide adenine dinucleotide 2'-phosphate reduced tetrasodium salt hydrate (NADPH)	Sigma-Aldrich, Steinheim, Germany	Cosubstrate	I, II
Boric acid	Riedel-de Haën, Seelze, Germany	Reagent	II–IV
Chloroform	Sigma-Aldrich, Steinheim, Germany	Solvent	III
Dipotassium hydrogenphosphate	Amresco, Solon, OH, USA	Reagent	I, II
Formic acid	Sigma-Aldrich, Steinheim, Germany	Reagent	I, IV

(Table 2 continues)

Chemical/Material	Manufacturer/Supplier	Note	Publication
Human liver microsomes (HLM), pooled from 20 donors	Corning, Wiesbaden, Germany	Enzyme product	I, II
Human liver microsomes (HLM), single donor	Corning, Wiesbaden, Germany	Enzyme product	II
Insulin receptor peptide (1142–1153), nonphosphorylated (IR0)[a]	Anaspec, Fremont, CA, USA	Standard	IV
Insulin receptor peptide, monophosphorylated (IR1A)[a]	Anaspec, Fremont, CA, USA	Standard	IV
Insulin receptor peptide, monophosphorylated (IR1B)[a]	Anaspec, Fremont, CA, USA	Standard	IV
Insulin receptor peptide, triply phosphorylated (IR3)[a]	Anaspec, Fremont, CA, USA	Standard	IV
Magnesium chloride hexahydrate	Sigma-Aldrich, Steinheim, Germany	Reagent	I, II
Methanol	Sigma-Aldrich, Steinheim, Germany	Solvent	I, IV
Morphine hydrochloride	University Pharmacy, Helsinki, Finland	Standard	III
Perchloric acid	Riedel-de Haën, Seelze, Germany	Reagent	I, II
Potassium dihydrogenphosphate	Riedel-de Haën, Seelze, Germany	Reagent	I, II
Sodium phosphate dibasic dihydrate	Sigma-Aldrich, Steinheim, Germany	Reagent	III
Sodium phosphate monobasic dihydrate	Sigma-Aldrich, Steinheim, Germany	Reagent	III
Trizma® base	Sigma-Aldrich, Steinheim, Germany	Reagent	I, II
Water (Milli-Q)	Millipore, Molsheim, France	Solvent	I–IV

[a] IR0: TRDIYETDYYRK; IR1A: TRDIpYETDYYRK; IR1B: TRDIYETDpYYRK; IR3: TRDIpYETDpYpYRK; T: threonine; R: arginine; D: aspartic acid; I: isoleucine; Y: tyrosine; E: glutamic acid; K: lysine; p: phosphorylated amino acid

Table 3. *CYP probe substrates, metabolites, and specific inhibitors. The probes recommended by the FDA [148] are written in italics.*

Enzyme	Substrate	Metabolite	Publication
CYP1A2	*Phenacetin*	*Paracetamol*	I
	3-Cyano-7-ethoxycoumarin (CEC)	3-Cyanoumbelliferone (CHC)	II
CYP2A6	*Coumarin*	*Umbelliferone*	I, II
CYP2B6	7-Methoxy-4-trifluoro-methylcoumarin (7-MFC)	7-Hydroxy-4-trifluoro-methylcoumarin (7-HFC)	II
CYP2C19	7-Methoxy-4-trifluoromethyl-coumarin (7-MFC)	7-Hydroxy-4-trifluoromethyl-coumarin (7-HFC)	II
CYP2D6	*Bufuralol*	*1'-Hydroxybufuralol*	I
	Luciferin-ME EGE	Luciferin-EGE[a]	I
	AMMC	AMHC	II
CYP2E1	7-Methoxy-4-trifluoromethyl-coumarin (7-MFC)	7-Hydroxy-4-trifluoromethyl-coumarin (7-HFC)	II
CYP3A4	*Testosterone*[b]	*6β-Hydroxytestosterone*	I
	7-Benzyloxyresorufin	Resorufin	II
	Dibenzylfluorescein	Fluorescein	II

[a] D-Luciferin is formed after deesterification of Luciferin-EGE by the esterase included in the Luciferin detection reagent of P450-Glo™ CYP2D6 Assay Kit (Promega).

[b] FDA recommends that two different substrates that are not structurally related are used for studying CYP3A4 inhibition.

ME: methyl ether; EGE: ethylene glycol ether; AMMC: 3-[2-(*N*,*N*-diethyl-*N*-methylammonium)ethyl]-7-methoxy-4-methylcoumarin; AMHC: 3-[2-(*N*,*N*-diethyl-*N*-methylammonium)ethyl]-7-hydroxy-4-methylcoumarin; N/A: not applicable.

3.2 SAMPLE PREPARATION

3.2.1 ENZYME INCUBATIONS

The CYP probe reactions recommended by FDA (Table 3) and a validated LC-MS method were used to study the effects of nanoformulations on the enzyme activities and clearances (I). The dose-dependent inhibition of CYP2D6 by the nanoparticles was further investigated using luciferin-based probe reaction. The fluorogenic CYP substrates were used in study of individual differences in enzyme activities (II).

The incubation conditions for CYP model reactions in liquid phase are listed in Table 4. The probe substrates were diluted in the incubation buffer, except for testosterone (5% (V/V) methanol left in reaction mixture) and CEC (2% (V/V) acetonitrile left in reaction mixture), which did not dissolve in purely aqueous solution. The substrate and the HLM were preincubated at 37 °C for 5 min before initiating the reaction by the addition of NADPH (1 mM

in reaction). The reaction mixture was incubated at 37 °C for the specified time after which the reaction was terminated by adding the quenching solution. The samples (except luminescence-based reactions) were placed on ice for at least 10 min after which the precipitated HLM was removed by centrifugation (16,000 g, 10 min) and the supernatant was collected for analysis. The luminescence-based samples were allowed to stand still in room temperature until measurement 20 min after addition of the quenching solution. The enzymatic reactions were performed in a total volume of 100 µL. Samples were analyzed without further sample treatment by LC-MS (I), luminescence (I), or fluorescence (II) depending on the metabolite.

Effects of nanoparticles and polymers

The enzyme kinetic parameters were determined for four CYP enzymes, CYP3A4, CYP2D6, CYP1A2, and CYP2A6, with testosterone, bufuralol, phenacetin, and coumarin as probe substrates, respectively (I). The enzyme activities (V_{max}), the Michaelis constants (K_m), and the intrinsic clearances (CL_{int}) were compared in the presence of three types of PSi nanoparticles and without them. The studied nanoparticles were alkyne-terminated thermally hydrocarbonized PSi (Alkyne-THCPSi), aminopropylsilane-modified thermally carbonized PSi (APTES-TCPSi), and thermally carbonized PSi (TCPSi). The reactions were performed as described above with seven different substrate concentrations. The nanoparticles (1 mg/mL in reaction) were added to the reaction mixture before preincubation step, and removed after the reaction together with the precipitated HLM by centrifugation. The effect of nanoparticle dose on CYP2D6 activity was studied using Luciferin-ME EGE as substrate. Seven different concentrations (1 ng/mL–1 mg/mL) of each type of nanoparticles were compared to control samples without nanoparticles. Comparison of the enzyme kinetic parameters in the presence of three polymers (0.1% m/V in reaction) was conducted similarly as with the nanoparticles. The selected polymers, Pluronics F68 and F127, and polyvinyl alcohol (PVA), are commonly used in the nanoformulations together with the PSi nanoparticles.

Incubations of the substrates and metabolites (one concentration) with each nanoparticle type were also performed without enzymes to distinguish the adsorption from enzyme inhibition. To study the adsorption effects in more detail, bufuralol and 1'-hydroxybufuralol were incubated with each nanoparticle type with different concentrations. Similarly, testosterone and 6β-hydroxytestosterone were studied in more detail in the presence of Alkyne-THCPSi. The observed free fractions were taken into account in calculating the enzyme kinetic parameters.

Table 4. *Incubation conditions for CYP model reactions.*

	CYP1A2		**CYP2A6**	**CYP2D6**		**CYP3A4**
Substrate	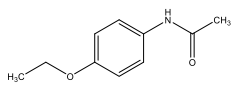 Phenacetin	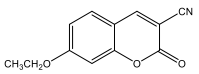 CEC	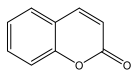 Coumarin	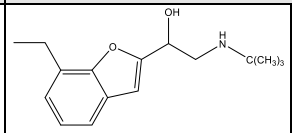 Bufuralol	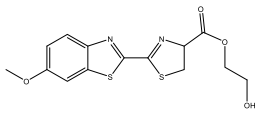 Luciferin-ME EGE	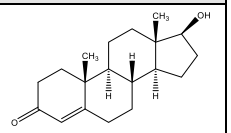 Testosterone
Metabolite	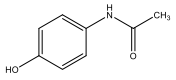 Paracetamol	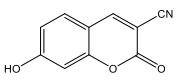 CHC	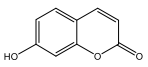 Umbelliferone	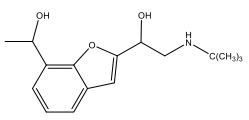 1'-OH-bufuralol	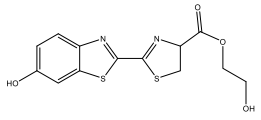 Luciferin-EGE	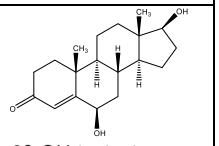 6β-OH-testosterone
Reaction in solution						
Buffer	Phosphate	Tris	Tris	Phosphate	Phosphate	Phosphate
Enzyme	0.8 mg/mL	0.8 mg/mL	0.4 mg/mL	0.8 mg/mL	0.4 mg/mL	0.5 mg/mL
Time	20 min	20 min	15 min	20 min	30 min	10 min
Quenching	Perchloric acid	ACN	Perchloric acid	Perchloric acid	Luciferin detection reagent	Perchloric acid
Ex/em	N/A	413/454 nm	355/447 nm	N/A	N/A	N/A
Reaction on µPAD						
Buffer	N/A	Tris	Tris	N/A	N/A	N/A
Enzyme	N/A	30 µg	30 µg	N/A	N/A	N/A
Time	N/A	30 min	30 min	N/A	N/A	N/A
Ex/em	N/A	428/463 nm	367/447 nm	N/A	N/A	N/A

CEC: 3-Cyano-7-ethoxycoumarin; CHC: 3-Cyanoumbelliferone; Phosphate: 0.1 M Potassium phosphate buffer (pH 7.4) with 3.3 mM $MgCl_2$; Tris: 0.1 M Tris buffer (pH 7.5) with 3.3 mM $MgCl_2$; Perchloric acid: 10% of reaction volume ice-cold 4 M perchloric acid is added to terminate the reaction; ACN: Equal volume (100% of reaction volume) of acetonitrile is added to terminate the reaction; Luciferin detection reagent: Equal volume (100% of reaction volume) of Luciferin detection reagent with esterase (Promega) was added to terminate the CYP mediated reaction and to catalyze the deesterification of luciferin-EGE to D-luciferin; Ex/em: Excitation/emission maxima; N/A: Not applicable.

3.2.2 PRETREATMENT OF PLASMA AND BRAIN SAMPLES

An MCE-EC method was developed and applied to analysis of morphine in mouse plasma and brain homogenate samples (III). The mice were administered 20 mg/kg morphine hydrochloride intraperitoneally (*i.p.*). After 30 min, the mice were sacrificed and the trunk bood was collected. The brains were dissected and homogenized in 5 mL of ice-cold water.

The samples were treated with liquid-liquid extraction (LLE) adopted with modifications from a previous study.[149] First saturated ammonium sulfate solution was added slowly to the sample and the mixture was centrifuged. The supernatant was collected and mixed with 0.1 M Na_2HPO_4 (pH 8.9) after which the mixture was extracted with chloroform–isopropanol (9:1) by vortex mixing. The organic phase was collected and the extraction was repeated. Finally, the organic phase was evaporated to dryness and the residue was dissolved in 5 mM MES buffer (pH 6.0) upon heating at 37 °C. The extraction resulted in 2-fold enrichment of plasma samples and 16-fold enrichment of brain homogenate samples.

3.2.3 DERIVATIZATION OF PHOSPHOPEPTIDES

An MCE-ESI/MS method was developed for separation of phosphorylated peptides according to the number of phosphorylated amino acid residues. To enable separation of the two monophosphorylated peptide isomers (IR1A and IR1B), two different derivatization protocols were used with either 9-fluorenylmethyl chloroformate (Fmoc-Cl) or 9-fluorenylmethyl *N*-succinimidyl carbonate (Fmoc-OSu) as the derivatization reagent. Fmoc-Cl was used in stoichiometric ratio or in 5 or 10-fold molar excess relative to the free amino residues of the peptide. Reactions were performed by mixing 20 µL of Fmoc-Cl (in ACN) with 10 µL of 18 mM sodium borate (pH 10.0) and 10 µL of peptide stock solution (1 mM in Milli-Q water). The mixtures were vortexed for 1 min and the reactions were left to proceed at room temperature for 2 min, 5 min, or 10 min. Fmoc-OSu was used in 10-fold molar excess and the reactions were initiated by mixing 10 µL of Fmoc-OSu (in ACN) with 10 µL of 18 mM sodium borate (pH 10.0) and 20 µL of peptide stock solution (1 mM in Milli-Q water). The reactions were left to proceed at room temperature overnight. After specified reaction time, the reaction mixtures were diluted for analysis.

3.3 ANALYTICAL METHODS

The most important instruments used in the study are listed in Table 5. Notes indicate their use.

Table 5. *Instruments used in the study.*

Instrument (model)	Manufacturer/supplier	Note	Publication
High voltage power supply and bipotentiostat (HVStat)	MicruX Technologies, Oviedo, Spain	MCE-EC control	III
Hybrid glass/SU-8 microchips (Pt-001T)	MicruX Technologies, Oviedo, Spain	Microchip for MCE-EC	III
Hybrid glass/SU-8 microchips (custom-designed)	MicruX Technologies, Oviedo, Spain	Microchip for MCE-EC	III
Ion trap mass spectrometer (6330)	Agilent Technologies, Santa Clara, CA,USA	Mass analysis	IV
Liquid chromatograph (ACQUITY UPLC™)	Waters, Milford, MA, USA	Sample separation	I
Power supply	Micralyne, Edmonton, Canada	MCE voltage supply	IV
Q-TOF mass spectrometer (Xevo)	Waters, Manchester, UK	Mass analysis	I
Varioskan Flash Multimode Reader	Thermo Fisher Scientific, Rockford, IL, USA	UV, luminescence	I
Varioskan Lux Multimode Reader	Thermo Fisher Scientific, Rockford, IL, USA	Fluorescence	II

3.3.1 LIQUID CHROMATOGRAPHY-MASS SPECTROMETRY

LC-MS measurements in publication I were performed with electrospray ionization in positive ion mode using an ACQUITY UPLC™ chromatograph and a Xevo Q-TOF mass spectrometer. The detailed LC-MS parameters are given in the supplement of publication I. The analytical method was validated for specificity, linearity, limits of detection and quantitation, and repeatability according to the ICH guidelines.[89]

3.3.2 MICROFLUIDIC PAPER-BASED DEVICE

A microfluidic paper-based assay was applied to analysis of individual CYP enzyme activities. The μPAD platforms were fabricated similarly as described previously in references [150] and [151]. Briefly, the functionalized calcium carbonate (FCC) with microfibrillated cellulose as a binder was applied on top of a polypropylene sheet to form a ca. 140 μm thick coating. Two layers of AKD ink mixed with yellow dye (wood stain colorant 157) was printed to create hydrophobic walls defining the main design. A semipermeable barrier was created by printing 4 layers of polystyrene mixed with red dye (Sudan Red G).

The assay design consists of different zones for each step of the protocol (Figure 6): The enzyme incubation is performed in the reaction area which is separated from the separation channel by the semibarrier which prevents leakage of the reaction mixture to the channel during the incubation. After the

incubation is completed, the reaction products are eluted through the semibarrier to the separation channel and finally to the tip where the fluorescent products can be detected. In addition, the assay includes the buffer reservoir area where an adsorbent pad is added during the incubation step to ensure that the reaction area stays wet. The multiplexed assay consists of 24 parallel assays and is designed to be compatible with a conventional well-plate reader. For fluorescence measurement, the μPAD platform was attached directly on top of the 384-plate adapter of the well-plate reader and aligned with help of light from below so that each tip of the platform was in the middle of a well.

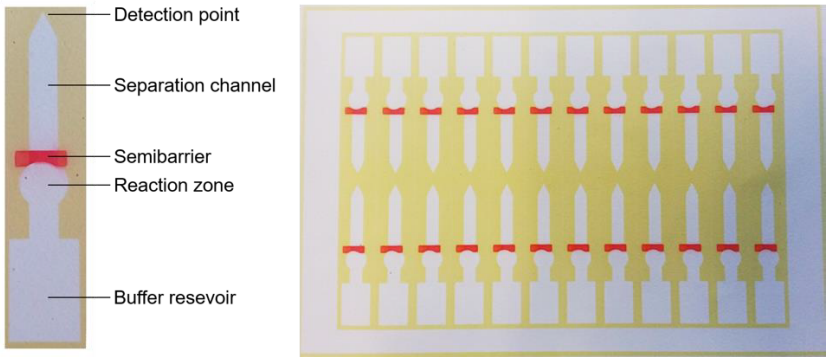

Figure 6 The FCC platform used in the study. Left: single assay and the different operational zones. Right: The multiplexed platform with 24 parallel assays.

Optimization of elution and detection

The retention factors (R_f) were determined by applying high concentrations of the metabolite standards or NADPH to the reaction spots and let dry for 15 min. The samples were eluted with elution buffer. The elution volumes were varied between 25 and 60 μL. An hour after elution, the assay was examined under UV lamp and the elution distance and band width were measured. To determine the optimal time point for detection, the metabolite standards were applied to the reaction areas and eluted as above. The fluorescence signals were measured every 10 min after elution up to 70–180 min and then with longer time intervals up to even 48 hours. The measurement was performed both at room temperature for the whole time and at 37 °C for first 6 hours and then at room temperature for the rest of the time. The LODs were roughly estimated by applying small amounts of each metabolite on a ring pattern (a circle with hydrophobic edges, detection without elution) and by measuring the fluorescence signals. The signals were compared to background signal to roughly estimate the LOD.

Enzyme incubations on-chip

The enzyme incubations on the µPAD were performed either at room temperature or at 37 °C. In the latter case, the µPAD assay platform was prewarmed on a hot plate to 37 °C. First, 1.5 µL of a mixture containing both the substrate and the cosubstrate (NADPH) in 0.1 M Tris buffer (pH 7.5) including 3.3 mM $MgCl_2$ was applied to the reaction area and let dry for ca. 5 min. The adsorbent pad was prewetted in the same incubation buffer and placed on the buffer reservoir area. When the liquid front reached the edge of the reaction area, 1.5 µL of HLM solution (20 mg/mL) was added to the reaction area. The addition of the enzyme was considered as the starting point of the reaction. During the incubation, more buffer was added to the adsorbent pad if necessary to keep the reaction area wet. After the specified incubation time, the adsorbent pad was removed and the assay was let dry for 15 min before elution with 60 µL of 20 mM borate buffer (pH 10). The fluorescence signals were measured after the assay was completely dry. The incubation conditions were optimized in terms of incubation time and amount of NADPH.

3.3.3 MICROCHIP ELECTROPHORESIS

Microchip electrophoresis (MCE) was used for analysis CYP substrates and metabolites [152], morphine in mouse plasma and brain samples (III), and phosphopeptides (IV). The designs of the different microchips are presented in Figure 7.

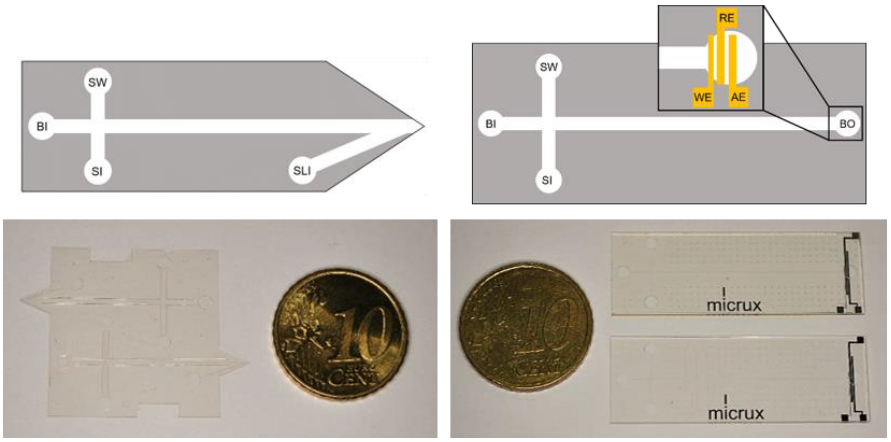

Figure 7 Schematic drawings (not in scale) and photographs of the microchips used in the study. Left: SU-8 microchip with ESI tip. Right: glass/SU-8 hybrid chips with straight and meandering separation channels. The platinum electrodes for amperometric detection are shown in the insert of the sketch. BI: buffer inlet; BO: buffer outlet; SI: sample inlet; SW: sample waste; SLI: sheath liquid inlet; WE: working electrode; RE: reference electrode; AE: auxiliary electrode.

Microchip electrophoresis-electrochemical detection

The commercial MCE-EC device (MicruX Technologies, Oviedo, Spain) consists of a high voltage power supply, a bipotentiostat, the hybrid glass/SU-8 microchip (Figure 7) with electrodes for EC detection, and a microchip holder with all necessary electrical connectors for applying the MCE and EC voltages. The channel cross-section of both injection and separation channel were 50 μm × 20 μm (width × height). The injection channel was 10 mm long, whereas the injection channel geometry and the length of the separation channel depend on the chip design. The three thin-film platinum electrodes were located in the buffer outlet close to the channel end with 100 μm spacing. The width of the working electrode (WE) was 50 μm, and the auxiliary electrode (AE) and the reference electrode (RE) were 250 μm wide each.

Before use, the microchip was filled and rinsed with background electrolyte (BGE). The samples were loaded electrokinetically (floating injection) by applying electric field between the sample inlet and the sample outlet (Figure 7). The electrophoretic separation was performed by applying an electric field between the buffer inlet and the buffer outlet. The electrophoretic and electrochemical detection voltages were controlled by the HVStat software provided together with the instrument.

For analysis of CYP metabolites, a custom-designed microchip (MicruX Technologies) with meandering separation channel (effective separation length, L_{eff} 50 mm) and off-set (50 μm) injection layout was used (Figure 7).[152] The BGE composition, WE potential, and sample loading time were optimized for best sensitivity. 20 mM borate buffer (pH 10.0) was selected as BGE for analysis of paracetamol, whereas 20 mM MES buffer (pH 6.0) was used for umbelliferone. Optimal WE potential was 1 V for both metabolites. LOD, LOQ, selectivity, linearity, run-to-run precision, and day-to-day precision was determined for both paracetamol and umbelliferone in optimized conditions. To increase the sensitivity, the paracetamol was diluted in 10 mM buffer (compared to 20 mM in BGE) and injected directly to the separation channel (electric field between SI and BO) followed by sample stacking during the separation step. The volume of the sample plug injected to the separation channel depends on the loading time, which was varied between 10 and 40 s.

Analysis of morphine samples (III) was performed with a standard commercial microchip with straight separation channel (L_{eff} 30 mm) and simple injection cross (Figure 7). 20 mM MES buffer (pH 6.5) was selected as the BGE, whereas the samples were diluted in 5 mM MES buffer (pH 6.0) which enabled additional concentration of the analytes by electrokinetic stacking during the separation step. The BGE composition, the separation voltage, and the WE potential were optimized for best selectivity and sensitivity. The robustness of the method was determined in terms of the loading time and the sample volume applied to the sample inlet. The method details are described in publication III. The method qualification was

performed by adopting the FDA Guidance for Industry – Bioanalytical Method Validation in relevant parts.[153] Lower limit of morphine quantitation (LLOQ), calibration curve, and between-run precision were determined with morphine standards in MES buffer. Selectivity, within-run precision, accuracy, and recovery were determined using blank plasma or blank brain homogenate sample spiked with known morphine concentrations. The recoveries and preconcentration factors (by LLE) were taken into account in calculation of the unknown morphine concentrations in animal samples.

Microchip electrophoresis-electrospray ionization mass spectrometry

The microchips with electrospray emitter tip were fabricated of SU-8 epoxypolymer as described in publication IV and in references [85] and [154] (Figure 7). The microchip comprised of a 25-mm long separation channel (50 μm × 50 μm, w×h, L_{eff} 20 mm) intersected by a 10-mm-long injection channel (simple cross), and a 12-mm-long auxiliary channel (100 μm × 50 μm, w×h) providing sheath liquid to the integrated ESI emitter tip. Small polydimethylsiloxane (PDMS) sheets with 2 mm inlet holes were placed on top of the SU-8 chip to avoid sample spreading on the relatively hydrophilic SU-8 before use. The microchip was filled and rinsed with water/methanol solution containing 40–60% (V/V) methanol and 20–40 mM ammonium acetate (BGE).

Samples were loaded in pinched injection mode by applying an electric field between the sample inlet and the sample outlet, and a small focusing potential to the buffer inlet. The sheath liquid inlet was left floating during injection and thus no spray was produced. The electrophoretic separation was performed in cathodic mode by applying high voltage to the buffer inlet. The ESI voltage applied to the sheath liquid inlet also served as the counter voltage for MCE separation. Small push-back voltages were applied to the sample inlet and the sample outlet during the separation step to prevent sample leakage to separation channel. An external power supply (Micralyne, Edmonton, Canada) was used to apply the voltages through platinum wires that were placed on the microchip inlets.

The Agilent 6330 ion trap mass spectrometer was equipped with an xyz-alignment stage to replace the standard ion source. The SU-8 microchip was placed on the xyz-stage in front of the MS inlet. The mass spectrometer was operated in positive ion mode with a capillary voltage of -1.6 kV. An ESI voltage of 2.0–3.2 kV was applied to the sheath liquid inlet. The sheath liquid was methanol–water 80:20 (v/v) containing 1% (v/v) acetic acid. The excess separation current was led to ground via a 50 MΩ resistor that was coupled in parallel with the ES voltage supply.

4 RESULTS AND DISCUSSION

In the following chapters, the main results are presented and discussed in view of the aims of the thesis. Further details can be found in the original publications (I–IV) and the related supporting information files.

4.1 DRUG METABOLISM AND PRECISION MEDICINE

4.1.1 EFFECT OF POROUS SILICON NANOPARTICLES ON CYTOCHROME P450 METABOLISM (I)

Nanoparticles are increasingly studied as new targeted, drug delivery methods in precision medicine. The safety of the nanoparticles is explored in terms of e.g., cytotoxicity, immune response, and biodegradation or accumulation in the body [155,156], but the effects on CYP enzymes are commonly neglected. Still, nanoparticles are known to accumulate in liver [157], where the CYP enzymes are also located. Few studies of gold and silver nanoparticles have shown potential interactions [158], but the porous silicon (PSi) nanoparticles have not been studied before. The properties of the studied nanoparticles are presented in Table 6.

In this study the Michaelis-Menten kinetics were determined for four CYP enzymes with probe substrates recommended by the FDA: CYP1A2 (phenacetin *O*-deethylation), CYP2A6 (coumarin 7-hydroxylation), CYP2D6 (bufuralol 1'-hydroxylation), and CYP3A4 (testosterone 6β-hydroxylation). Out of these enzymes, CYP2D6 was most vulnerable to inhibition by all three types of nanoparticles. The enzyme activity (V_{max}) was clearly decreased in the presence of each nanoparticle type even after corrections of the adsorption effects, whereas only minor changes in the Michaelis constant (K_m) and intrinsic clearance (CL_{int}) were observed (Figure 8). The CYP3A4 activity was slightly decreased in the presence of APTES-TCPSi and TCPSi, but only in the latter case a decrease in CL_{int} was observed. Addition of Alkyne-THCPSi resulted in increase of both V_{max} and K_m of testosterone hydroxylation by CYP3A4, but the CL_{int} was not affected. Both V_{max} and K_m of phenacetin *O*-deethylation by CYP1A2 were decreased in the presence of all nanoparticle types. However, the CL_{int} values for CYP1A2 in the presence of APTES-TCPSi and Alkyne-THCPSi were actually increased compared to the control. The V_{max} of CYP2A6 was not affected by TCPSi, but the K_m was decreased resulting in increased CL_{int}. In turn, after addition of Alkyne-THCPSi the V_{max} was decreased, whereas K_m and CL_{int} remained in the same level with the control. APTES-TCPSi caused slight increase in V_{max} and CL_{int}.

Table 6. *Properties of the porous silicon nanoparticles (mean and standard deviation).*

	Alkyne-THCPSi	**APTES-TCPSi**	**TCPSi**
Surface charge	- 30 mV	+ 35 mV	- 30 mV
Hydrophilicity	Hydrophobic	Hydrophilic	Hydrophilic
Particle size	184 nm	176 nm	159 nm
Pore diameter	12.1 ± 1.2 nm	8.0 ± 0.7 nm	10.7 nm

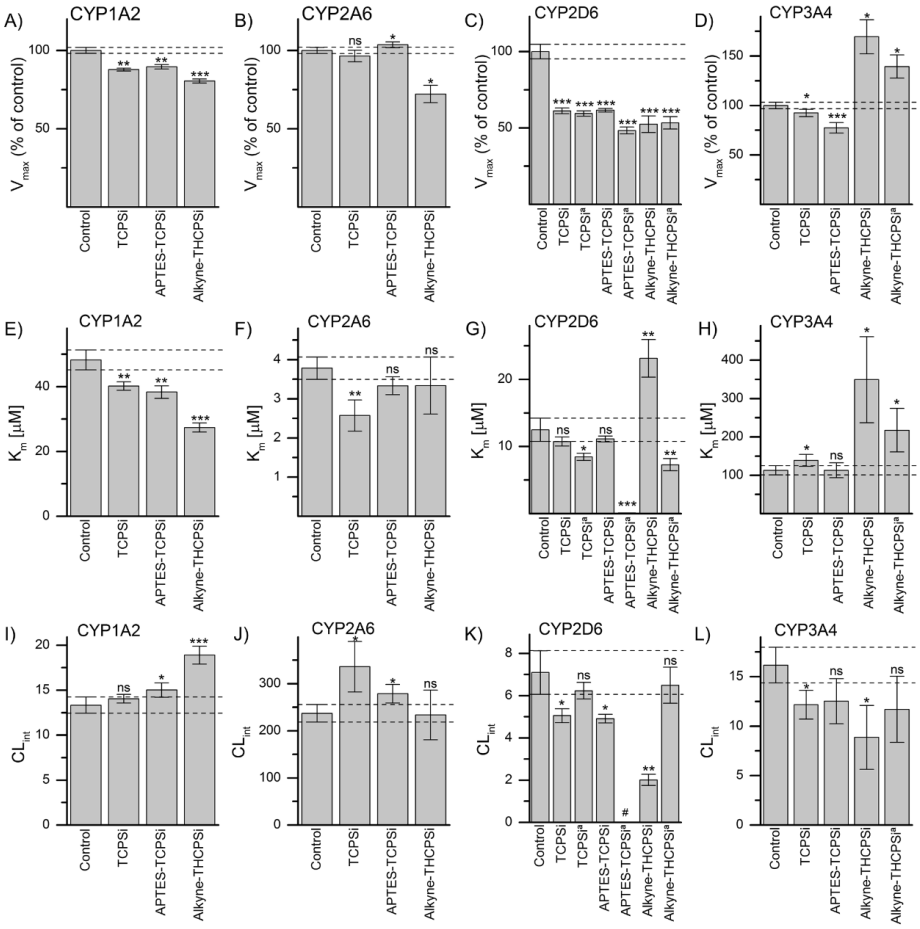

Figure 8 A-D) The maximum reaction rates (V_{max}) relative to control (adjusted to 100%), E-H) the Michaelis constants (K_m), and I-L) the intrinsic clearances (CL_{int}) of the CYP model reactions in the presence of the PSi nanoparticles. The error bars present the standard deviation (n = 4). The adsorption corrected values are marked by ([a]) after the name of the nanoparticle type. Results of Student's *t*-test with Welch's correction (above the bars): ***: $p < 0.001$; **: $0.001 < p < 0.01$; *: $0.01 < p < 0.05$; ns: not significant ($p > 0.05$). # The K_m was so small that the Michaelis-Menten fit was not able to reliably predict it and thus the CL_{int} could not be calculated. Adjusted with permission from ref. [159] originally published in European Journal of Pharmaceutical Sciences.

The effects of the nanoparticles on CYP2D6 were further investigated with seven different nanoparticle concentrations (1 ng/mL–1 mg/mL) and a luminescence-based model reaction. The inhibition by APTES-TCPSi remained in the same level despite the nanoparticle concentration. More dose-dependent inhibition was observed with the other two nanoparticle types, and the minimum inhibitory concentrations were 1 μg/mL for TCPSi and 10 μg/mL for Alkyne-THCPSi.

The three polymers investigated were block copolymers F68 and F127, and PVA, which are commonly used in nanoformulations together with the PSi nanoparticles. CYP2D6 was again most prone to inhibition (decreased V_{max}) by all the studied polymers, but the intrinsic clearances were increased by the block copolymers as a result of simultaneous decrease of K_m. The intrinsic clearance of CYP3A4 was not affected by any of the polymers, whereas V_{max} and CL_{int} of both CYP1A2 and CYP2A6 were increased by the block copolymers. PVA did not affect the intrinsic clearance of any enzyme.

While statistically significant decreases in enzyme activities were observed, the inhibition mechanisms are not that obvious. Based on the changes in V_{max} and K_m the different reversible inhibition mechanisms can be distinguished, but irreversible inhibition causes similar changes as noncompetitive reversible inhibition and is thus difficult to detect based on enzyme kinetic parameters. The average size of the nanoparticles varied in the range of ca. 160–180 nm, whereas the active site cavities of CYP enzymes are typically below 3 nm^3 in size.[160] Competitive binding to the active size is thus not likely. In addition, the cellular uptake of PSi nanoparticles by hepatocytes remains to be characterized in the future. However, the results indicate that the possibility of interactions should be studied also in vivo. CYP2D6 was shown to be the most vulnerable to inhibitory effects and as it is also highly polymorphic enzyme, the inhibitory effects may cause even stronger effects in populations with intrinsically lower CYP2D6 activity. Also, the combinatory effects of the nanoparticles and polymers are of interest, as they may either reinforce or compensate each others' effects.

4.1.2 MICROFLUIDIC PAPER-BASED DEVICE FOR STUDYING INDIVIDUAL DIFFERENCES IN CYTOCHROME P450 ACTIVITY (II)

The individual differences in CYP activities may be caused by polymorphic differences in the corresponding genes. These differences can be studied with genetic tests, which are relatively simple and fast, as described in the chapter 1.1.3. However, also other than genetic factors can have significant effects on CYP activities, as described above in terms of the nanoformulations. These effects should also be considered as they can have equally strong impact on the safety and efficacy of the medication. The currently existing methods for studying the effects of the nongenetic factors are slow and laborious. The aim of this study was to develop a simple microfluidic platform for screening of individual differences in CYP enzyme activities. Instead of traditional

chromatographic paper, a paper-like coating based on FCC was used. The FCC coating was previously shown to be biocompatible material with low optical background and easily controlled wetting properties.[150] The characterization and optimization of the FCC coating and the assay design have been published by Jutila et al.[150] Also, activity of CYP enzymes on the μPAD device was preliminarily demonstrated.

In this study, the assay was multiplexed and detection with conventional well-plate reader was investigated to enable simple and fast read-out. The assay was applied to analysis of individual differences in CYP enzyme activities. The CYP activities were studied with fluorogenic probe substrates (producing fluorescent metabolites) [161–163] instead of those recommended by the FDA. For a simple assay, easy readout is also required and the use of the fluorogenic substrates enabled fluorescence detection, which was not applicable for the reactions recommended by the FDA.

Optimization of elution and detection

Fluorescent metabolites of six different CYP model reactions were preliminarily characterized for their suitability to enzyme activity screening on FCC platform. The assay consists of a reaction zone and a detection point separated by a semibarrier and separation channel. This enables separation of the metabolites produced in the reaction area from the CYP enzymes and NADPH, which may interfere with the fluorescence detection especially close to the UV range. The elution of the metabolites was examined by measuring the R_f values with different elution buffers and elution volumes (Table 7). In addition to efficient elution of the metabolite to the tip, the elution buffer affected to the detection of the metabolites and to the retention of the cosubstrate NADPH to the FCC. Borate buffer (20 mM, pH 10.0) was found optimal for elution and detection of all metabolites, except fluorescein, which was retained to the FCC coating through the whole separation channel. Phosphate buffer (pH 12) was the only buffer that enabled elution of fluorescein to the tip, but unfortunately it affected the FCC coating and the hydrophobic barriers, resulting in leakage from the hydrophilic areas to the hydrophobic areas. Thus, phosphate buffer could not be used, whereas in the other tested buffers (Tris buffer pH 7.5 or pH 9, MES buffer pH 6.5) fluorescein was not fluorescent, and it was excluded from further studies. After selection of the buffer, the elution volume was optimized for each metabolite. The minimum volume required for elution was previously determined to be 25 μL [150], while the maximum volume hold by the hydrophobic AKD barriers was found to be 60 μL.

Table 7. *Optimized parameters on µPAD for the fluorescent CYP metabolites.*

Enzyme[a]	Substrate	Metabolite	Retention factor[b]	LOD	Ex/em (nm)
CYP3A4	7-Benzyloxy-resorufin	Resorufin	0.66 ± 0.13	0.02 pmol	579 / 597
CYP1A2	CEC	CHC	0.77 ± 0.14	0.2 pmol	428 / 463
CYP2B6	7-MFC	7-HFC	0.59 ± 0.09	2 pmol	398 / 477
CYP2A6	Coumarin	Umbelliferone	0.91 ± 0.09	2 pmol	367 / 447
CYP2D6	AMMC	AMHC		2 pmol	382 / 447

[a] Only the CYP enzyme with highest activity in metabolism of the substrate is listed.

[b] R_f value was measured 1 hour after elution by 25 µL of borate buffer.

The detection was optimized by eluting the metabolites to the detection point in the tip of the channel (Figure 6) and by measuring the fluorescence signal with regular intervals until a stable signal was reached. The measurements were performed at RT and at 37 °C. The results showed clear increase in the fluorescence signal immediately after elution as the metabolites eluted to the tip. The maximal signal intensity was achieved between 20 and 80 min depending on the R_f value of the metabolite and the temperature (RT or 37 °C) which affected the capillary filling and evaporation rates. The signals of resorufin and 7-HFC remained stable after reaching the maximum for at least 23 hours despite the evaporation of the liquid, whereas the signals of the other umbelliferone derivatives decreased rapidly after reaching the tip upon drying of the assay. Figure 9 shows the variation of the signal intensity after elution of umbelliferone and CHC. The time from elution to the maximal signal varied also depending on the metabolite concentration, and thus the assay readout was impractical in wetted state. Instead, the method was developed aiming at detection of the metabolites in dry state. After drying, the signal was stable at least up to 23 hours also in case of the umbelliferone derivatives.

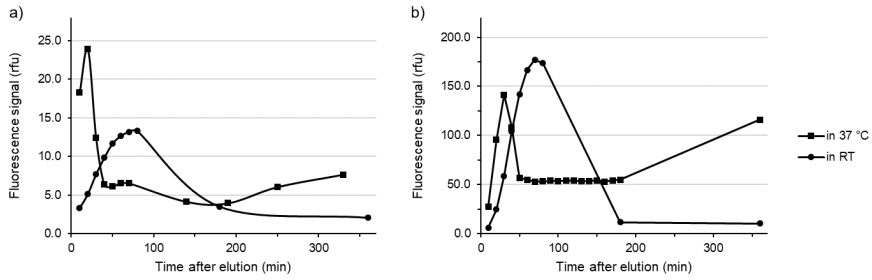

Figure 9 The effect of time on fluorescence signal of a) umbelliferone and b) cyanoumbelliferone (CHC) at room temperature (RT) and at 37 °C.

The LOD of resorufin was shown to be only few tens of femtomoles, whereas the LODs of umbelliferone derivatives were in the range of few picomoles. The background signal derived from the assay platform itself increased as the excitation and emission wavelengths were decreased, which explains the higher background signal and thus decreased sensitivity of the umbelliferone derivatives. The estimated LODs are listed in the Table 7. Despite the better LODs before elution, the detection was not possible in these conditions in the enzymatic assays due to the background signal caused by other reaction components, and thus elution (separation) was necessary.

Optimization of enzyme incubation conditions

The enzyme incubation conditions were optimized in terms of incubation temperature, NADPH amount, and incubation time. However, only the reactions mediated by CYP1A2 (CEC as substrate) and CYP2A6 (coumarin as substrate) produced sufficiently high amounts of the metabolites, CHC and umbelliferone, to enable accurate detection on the μPAD. Even resorufin, which had lower LOD than any of the other metabolites, was not formed in sufficiently high amounts. This was likely because of the turnover of 7-benzyloxyresorufin to resorufin is reported to be low [161], although the molecular properties of the substrate may also complicate the assay. For example, the substrate, 7-benzyloxyresorufin, is poorly soluble in water and it was thus applied to the reaction area in solution containing 5% of DMSO, which is likely to decrease the enzyme activity.[164] On the other hand, if all DMSO was evaporated, the poor solubility of the substrate may also limit the redissolution of the substrate to the incubation buffer.

The reactions of coumarin and CEC were studied at RT and at 37 °C. The CYP1A2 activity was not significantly altered by the incubation temperature, whereas the activity of CYP2A6 was higher at 37 °C as expected. However, further reactions were conducted at RT, because in these conditions smaller deviations were obtained (Figure 10a). The large variation at 37 °C is most likely result of uneven drying of the assays during the incubation. In these conditions, the evaporation is faster and the assays may dry out unless incubation buffer is added to the adsorbent pad during the incubation.

The amount of cosubstrate NADPH should be high enough not to limit the reaction rate. Thus, the NADPH amount was optimized with CYP2A6 probe reaction (Figure 10b). As expected, the enzyme activity was increased when the amount of NADPH was increased from 1.5 nmol to 3.75 nmol, whereas further increase to 7.5 nmol did not increase the activity notably. The metabolite production could not be measured with NADPH amounts higher than 7.5 nmol, because the capability of the FCC coating to retain NADPH was exceeded and NADPH was eluted to the tip of the separation channel where it interfered with the detection of the metabolites. In further studies, 7.5 nmol of NADPH was used (corresponding to 5 mM concentration in the applied volume of 1.5 μL).

The incubation time was varied between 10 and 30 min at RT. Interestingly, a relatively small increase in metabolite production was observed for both CYP1A2 and CYP2A6 and the enzyme activities were actually decreased. (Figure 10c). Instead, a clear decrease in the background signal was observed as the incubation time increased (Figure 10d), especially at the wavelengths of umbelliferone detection. The origin of this background signal was related to incubation of NADPH, as the samples incubated without NADPH did not produce similar background signal, nor did nonincubated NADPH. The signal did not originate from NADPH itself because it did not elute to the tip. Thus, most probably NADPH reacts with the enzymes resulting in a fluorescent byproduct that is not retained by the FCC as strongly as NADPH itself. To maximize the metabolite production and the signal-to-noise ratio, incubation time of 30 min was selected for the final application. However, the almost equal metabolite production but smaller deviation would suggest that 20 min incubation time could improve the precision of the assay.

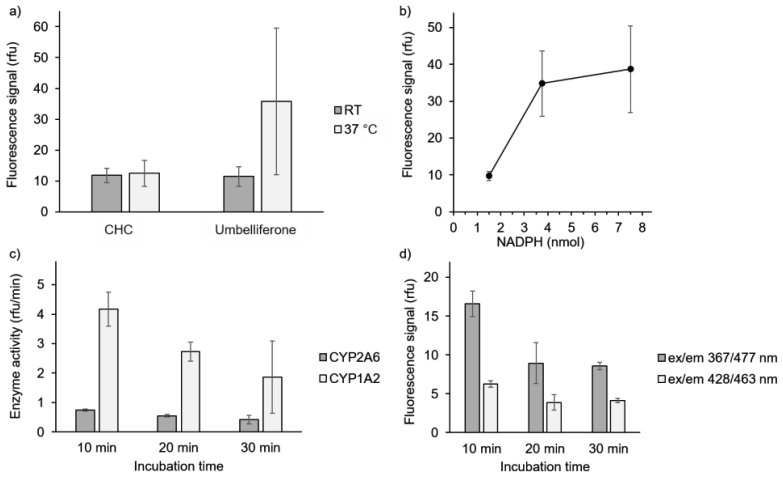

Figure 10 a) Effect of incubation temperature on activity of CYP1A2 (amount of CHC produced) and CYP2A6 (amount of umbelliferone produced). b) Effect of NADPH amount on production of umbelliferone by CYP2A6. c) Effect of incubation time on enzyme activity of CYP2A6 and CYP1A2. d) Effect of incubation time on background signal originating from NADPH by product on excitation and emission wavelengths used for detection of umbelliferone (367/477 nm) and CHC (428/463 nm). The error bars present the standard deviation (n = 3).

Individual differences in enzyme activities

The developed assay platform was applied to analysis of CYP1A2 and CYP2A6 activities in HLM of three individuals. The activities were compared to average activities in a 20-donor pool of HLM. The assays were designed in a way that it enabled simultaneous determination of both enzyme activities for one donor as well as the activities of pooled HLM on a single FCC platform with

24 parallel assays. In Figure 11, the enzyme activities of each donor determined by the µPAD assay and by a conventional in-solution assay (in-house), are presented relative to the pooled HLM (adjusted to 1, the dashed line). In addition, the values reported by the enzyme supplier are included for comparison. The supplier uses the same model reaction for determining CYP2A6 activity, but for CYP1A2 phenacetin *O*-deethylation is used.

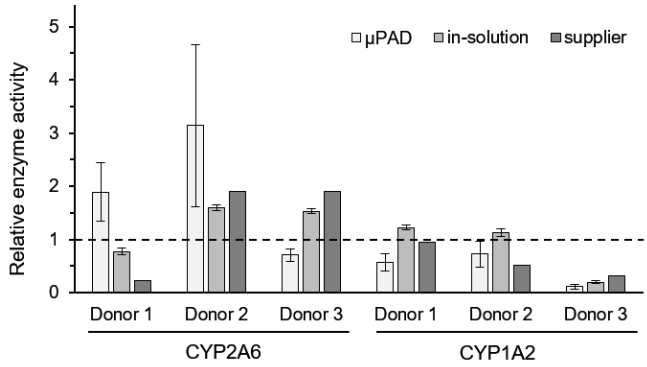

Figure 11 The CYP2A6 and CYP1A2 activities of the HLM from three different donors. The activities are presented as relative values compared to activity of pooled HLM (20 donors), which is adjusted to 1 (the dashed line). The activities were determined on the µPAD and in conventional in-solution assay (in-house) and compared to the activities reported by the supplier. The error bars show the standard deviation (n = 4).

The µPAD assay predicts markedly high CYP2A6 activity for donors 1 and 2, whereas donor 3 has slightly lower CYP2A6 activity compared to pooled HLM. The differences compared to pooled HLM determined by the in-solution assay are much smaller, but also opposite to those determined by the µPAD assay for donors 1 and 3. The observed CYP2A6 activities in the in-solution assay were similar to those reported by the supplier, which is expected as the same probe substrate and similar incubation conditions were used. The CYP1A2 activities predicted by the µPAD assay were low compared to the pooled HLM for all donors. The supplier also reports activities of the donors to be close to the activity in pooled HLM or lower, whereas the in-solution assay shows slightly increased activities for donors 1 and 2. The CYP1A2 activity of donor 3 is very low and similarly predicted by all the methods.

Based on the results, further validation and improvement in precision and robustness are required to fulfill the requirements for a reliable diagnostic assay. In case of CYP1A2, the key difference between the in-solution assays performed in-house and by the supplier, was the probe substrate. The supplier uses a FDA-recommended probe, phenacetin, which is metabolized selectively by CYP1A2, whereas here the fluorogenic CEC was selected. CEC is also metabolized mainly by CYP1A2 in the liver, but some contributions from CYP2C9 and CYP2C19 are expected.[161,165] It has also been noted that use

of different probe substrates may end up in different results, especially in enzyme inhibition studies.[166] Also, the experimental conditions affect significantly and should be very carefully optimized. For CYP2A6, the same probe substrate was used in all cases, so that cannot explain the differences. On μPAD, the high background signal complicated the interpretation of CYP2A6 activities, though this effects should be similar for both the individual donor samples and the pooled sample, and thus not affect the relative activities.

It can be concluded that at the current state, the FCC μPAD platform is not able to predict the enzyme activities with good enough reliability and robustness. However, the results clearly show that the CYP enzymes were active also on FCC at RT. Further optimization of the incubation protocol and conditions, as well as advances in the probe substrates are required before the developed platform can be used for real clinical analysis. Comparative studies of "conventional" probes recommended by the FDA and the fluorogenic probes have been conducted demonstrating the challenges of the fluorogenic probes.[162,167] Only few of these reactions are truly specific which complicates their use with HLM. In addition, the poor solubility of the substrates requires use of organic solvents which may result in enzyme inhibition even in amounts below 0.2% (V/V) in the reaction mixture.[164] Despite the challenges, the main reason for selecting fluorogenic probes over others, is typically the fast and simple readout of the fluorescence signal compared to e.g. LC-MS analysis. This was also aimed at in this study, as a more complex detection method would disable easy use e.g., in point-of-care applications and as a simple tool for precision medicine.

4.2 MICROCHIP ELECTROPHORESIS IN PHARMACEUTICAL ANALYSIS

In this thesis, MCE methods were developed for three different pharmaceutical applications. First, MCE-EC was applied to analysis of CYP metabolism aiming at increased throughput compared to conventional analytical methods. The same device was also applied to targeted quantitative analysis of morphine from biological samples. This is a very typical analytical task in pharmaceutical research to obtain pharmacokinetic and pharmacological information by analyzing a drug or its metabolites e.g. in plasma. However, behavioral studies are commonly limited to observations of the animal, e.g. locomotor activity, eating etc. A simple, commercial analytical device with easy operation without special expertise, could provide additional chemical information and improve the outcome of the studies. The third application aims to demonstrate the power of MCE in an analytical task that is commonly challenging for conventional methods. Protein phosphorylation plays a significant role in e.g. cell proliferation, differentiation, and apoptosis. Abnormal phosphorylation has been connected to many diseases including

diabetes and cancers.[168] However, analysis of phosphopeptides in protein digests is challenging due to the low abundance and poor ionization efficiency (in MS) of the phosphopeptides. Thus, an MCE-ESI/MS method was developed for separation of nonphosphorylated peptide from the phosphorylated forms of the same peptide. In addition, further derivatization step was included to enable separation of positional phosphorylation isomers.

4.2.1 ANALYSIS OF CYTOCHROME P450 METABOLISM

A commercial MCE-EC device was applied for analysis of FDA recommended CYP probe reactions.[152] Four metabolites, paracetamol (CYP1A2), umbelliferone (CYP2A6), 1'-hydroxybufuralol (CYP2D6), and 6β-hydroxytestosterone (CYP3A4), were preliminarily studied. However, only paracetamol and umbelliferone showed high enough electroactivity to be detected with the MCE-EC method.

The separation and detection conditions were optimized for both paracetamol and umbelliferone. The method showed good selectivity for both substrate-metabolite pairs: Coumarin was not electroactive with the selected WE potential and did not disturb the analysis of umbelliferone. Phenacetin (t_{migr} = 26.9 s) was detected in the selected conditions, but it was rapidly separated from paracetamol (t_{migr} = 37.2 s) by MCE. Phenacetin and paracetamol spiked in the enzyme incubation matrix (after termination of the reaction) could also be separated and detected with the same method without any additional clean-up steps. Both within-run and between-run precisions of the peak area were on acceptable level (Table 8). Detection and quantitation limits were in micromolar level determined from standard solutions. Based on the enzyme activities determined in publication I, the maximal amounts of paracetamol and umbelliferone formed in enzymatic reactions are approximately 10 μM and 5 μM, respectively. However, in study of enzyme kinetics or enzyme inhibition, detection of much lower concentrations is required. Thus, electrokinetic sample stacking was applied for analysis of paracetamol to enhance the detection sensitivity. The samples were prepared in more diluted buffer (compared to BGE) and injected to separation channel (electric field between sample inlet and buffer outlet). During the separation step, the decreased ionic concentration of the sample plug resulted in lower conductivity and higher electric field strength compared to BGE, and thus concentration of the negatively charged paracetamol to the end of the sample plug. By injecting the sample from sample inlet towards buffer outlet (instead of sample waste), the volume of sample plug was increased and determined by the loading time rather than channel geometry. Up to 3-fold increase of peak area was achieved with loading time of 15 s. Longer sample loading times resulted in large sample plugs in separation channel and significant peak broadening, and ended up in reduced sensitivity. Further optimization of sensitivity by e.g., additional sample concentration step before MCE, are required to enable CYP metabolism studies with the tested MCE-EC method

and the selected probes. Also model reactions with highly electroactive metabolites would improve the sensitivity and enable study of other CYP enzymes, including the most important drug-metabolizing enzymes CYP3A4 and the highly polymorphic CYP2D6.

Table 8. *The validation results of MCE-EC method for analysis of paracetamol and umbelliferone.*

Parameter	Paracetamol	Umbelliferone
Limit of detection	2.4 µM	3.9 µM
Limit of quantitation	7.4 µM	11.9 µM
Linear range	15–100 µM (R^2 = 0.98263)	15–100 µM (R^2 = 0.99067)
Within-run precision[a]	6.1% (CV)	10.4% (CV)
Between-run precision[b]	12.3% (CV)	n.d.

[a] 6 injections, sample concentration 50 µM.

[b] 3 injections on 3 different days, sample concentration 100 µM

CV: coefficient of variation; n.d.: not determined

4.2.2 ANALYSIS OF MORPHINE IN MOUSE PLASMA AND BRAIN (III)

The same commercial MCE-EC device described above was used to analyze morphine in mouse plasma and brain homogenate samples as a part of a behavioral animal study addressing morphine addiction. The separation voltage and WE potential were optimized and selected based on sensitivity and precision. Separation voltage of 1000 V (333 V/cm) enabled best separation efficiency and WE potential of 1 V provided highest sensitivity. Also, increase in sample volume applied to the sample inlet as well as increase in loading time increased the detected peak area. To further improve the peak shape, the ionic concentration of the sample buffer was decreased to 5 mM (20 mM in BGE) to enable further concentration of the sample during the separation step by electrokinetic sample stacking. The cationic morphine migrates faster in the sample plug concentrating in the front of the plug.

An off-chip LLE was performed before the MCE-EC analysis. The LLE method enabled 2-fold enrichment of morphine in plasma samples and 16-fold enrichment in brain homogenate samples by adjusting the sample volume and the final volume after LLE. The recovery of morphine from plasma samples was only 24–31%, which was probably affected by the relatively high fraction of morphine bound in plasma proteins.[169] However, the 2-fold enrichment during LLE compensated the low recovery. The recovery of morphine from brain homogenate samples was much better (69% for 1 µM morphine) as expected due to lack of plasma proteins.

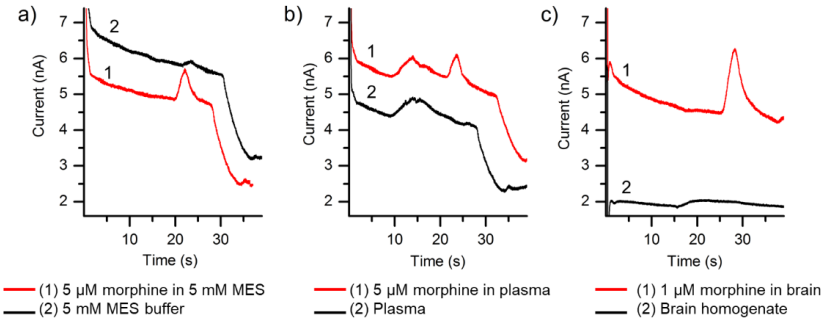

Figure 12 Electropherograms of morphine in different matrices compared with blank matrix. (a) 5 µM morphine in 5 mM MES buffer, (b) 5 µM morphine in mouse plasma, and (c) 1 µM morphine in mouse brain homogenate. Plasma and brain samples were treated with LLE before analysis and the residue was dissolved in 5 mM MES (pH 6.0) buffer after evaporating the extraction solvent. All separations were performed at 333 V/cm using 20 mM MES (pH 6.5) as the BGE and working electrode potential of 1.0 V. The. Reprinted from ref. [170] originally published in Scientific Reports licensed under CC-BY 4.0 https://creativecommons.org/licenses/by/4.0/.

The method was validated in terms of selectivity (Figure 12), linearity, limit of quantitation, within-run and between-run precision, and accuracy according to the FDA guidelines.[153] The validation results and the FDA requirements are presented in Table 9. The lower limit of quantitation (LLOQ) was 0.4 µM which corresponds to only 20 amol of morphine in the injected volume (50 pL based on the injection cross geometry). Within-run precision between 3.7 and 12.3% (CV, 6 injections on each concentration) was achieved for morphine in plasma samples, but the between-run precision (4 injections on 3 different days) were higher, especially at 1 µM concentration, where the method was not able to meet the FDA criteria. To overcome the deviation between days, the calibration curve was established separately on each day. The accuracy was also good at 5 and 20 µM concentrations, but again at 1 µM concentration the accuracy was slightly outside the FDA limits. However, the concentrations measured in this study, were above 5 µM and thus the method was considered suitable for quantitation of morphine in plasma. For morphine (1 µM) in brain homogenate within-run precision of 7.7% (CV) and accuracy of 89.6% was achieved.

The sensitivity was in a relatively good level and similar to that achieved in a previous study for morphine in urine samples.[103] The method applied in urine analysis was, however, not suitable for analysis of small volume samples, as an off-chip conventional solid-phase extraction was performed prior to MCE-EC analysis. Thus, in this thesis, LLE was selected as a sample preparation method because it is easily scalable based on the available sample volume. The volume of the plasma samples was only few tens of microliters, whereas the brains were homogenized in 5 milliliters of water. On the other hand, the morphine concentration in plasma was much higher than in the brain homogenate. The LLE method was suitable for both matrices as it

enabled higher enrichment factor for brain homogenate samples to reach concentrations above LLOQ in LLE-treated samples and treatment of plasma samples with less enrichment, but small volume.

Table 9. *Method validation results for analysis of morphine by MCE-EC.*

Parameter	Value	FDA criteria	OK?
Lower limit of quantitation[a] (n = 4)	0.4 µM (16.1% CV)	CV < 20%	OK
Linear range[a]	0.5–20 µM		
Coefficient of variation (n = 5)	1.1–10.9%	< 15%	OK
Deviation from nominal concentration	0.3–7.7%	< 15%	OK
Between-run precision of peak area (CV)[a] (n = 4 on 3 different days)			
1 µM	29.4%	< 15%	NO
5 µM	5.3%	< 15%	OK
20 µM	7.9%	< 15%	OK
Within-run precision of peak area (CV)[b] (n = 6)			
1 µM	12.3%	< 15%	OK
5 µM	3.7%	< 15%	OK
20 µM	4.5%	< 15%	OK
Accuracy[b] (n = 6)			
1 µM	119.2%	85–115%[c]	NO
5 µM	106.9%	85–115%	OK
20 µM	100.7%	85–115%	OK

[a] Determined from standard samples.

[b] Determined from spiked plasma samples.

[c] The FDA guideline requires that the mean value is within 15% of the actual value corresponding to accuracies 85–115%.

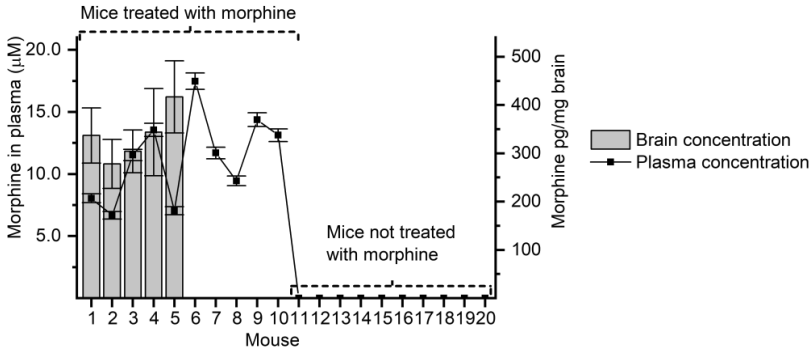

Figure 13 The detected morphine concentrations in plasma (scatter graph, left y-axis) and brain (bar graph, right y-axis) for each mouse. The mice no. 1–10 were administered morphine hydrochloride (20 mg/kg), whereas the mice no. 11–20 were not treated with morphine. The error bars represent propagated error based on precision and recovery. Revised from ref. [170] originally published in Scientific Reports licensed under CC-BY 4.0 https://creativecommons.org/licenses/by/4.0/.

One of the aims of this study was also to evaluate the feasibility of the commercial portable MCE-EC system for routine use in e.g., animal research facilities. The chemical information that could be easily achieved on-site, would offer additional data for behavioral animal studies. A targeted application could easily be optimized, as demonstrated in this study, to enable simple quantitative analysis. Also considering the use of the method outside analytical chemistry laboratory, LLE is more suitable sample preparation method as it does not require any additional instrumentation. Even integration of the LLE on the microchip could be feasible with e.g., similar method previously demonstrated for drug metabolism studies.[96]

The developed method was applied to analysis of mouse plasma and brain samples derived from a behavioral study. Plasma samples of 10 mice treated with morphine and another 10 mice without morphine treatment were analyzed. The morphine plasma concentrations were between 6.7 and 17 μM (Figure 13). No morphine was detected in the plasma of non-treated mice. The detected plasma concentrations were in line with previous studies.[171] In addition, brain homogenate samples of five mice treated with morphine were analyzed. The concentrations of morphine in brain followed the same trend as in plasma in four cases out of five.

4.2.3 SEPARATION OF PHOSPHOPEPTIDES (IV)

In publication IV, the MCE technology combined with ESI/MS detection was challenged in an analytical task commonly difficult for many conventional techniques. Analysis of phosphopeptides is difficult due to their low abundance in protein digestions and their poor ionization efficiency (compared to corresponding nonphosphorylated peptide) in electrospray. In addition, the positional phosphorylation isomers (same peptide with same number of phosphorylations but on different amino acid residues) are not possible to separate based on their mass/charge (m/z) ratio and even the interpretation of MS/MS spectra is commonly challenging. Insulin receptor peptide (IR0, amino acids 1142–1153 of the insulin receptor) was selected as a model compound with the corresponding peptides with one phosphorylation at tyrosine 1146 (IR1A) or at tyrosine 1150 (IR1B), and all three tyrosine residues (1146, 1150, and 1151) phosphorylated (IR3).

The separation conditions were optimized, including the separation voltage, ionic strength of BGE, and methanol content of the BGE. The selected BGE consisted of 40% of water and 60% of methanol (V/V) including 30 mM ammonium acetate (pH 7.4). The monophosphorylated peptides and the triply phosphorylated peptide were separated from the nonphosphorylated peptide at electric field strength of 750 V/cm in less than 40 s (Figure 14). The within-run precision of the migration times was 7.5–11.3% (CV, n = 5) without internal standard and 3.1–4.7% (CV, n = 5) with the nonphosphorylated peptide as internal standard. The nonphosphorylated peptide migrated at

20.0 ± 1.7 s, monophosphorylated peptides at 22.8 ± 1.7 s (single peak), and triply phosphorylated peptide at 27.5 ± 3.1 s (n = 5).

To enable separation of the monophosphorylated peptide isomers, a derivatization protocol was applied. The derivatization reagent, 9-fluorenylmethyl (Fmoc) binds to amino groups of the peptides. Insulin receptor peptide has four amino groups: two close to the N-terminal end (threonine and arginine), and two close to the C-terminal end (lysine and arginine). Both rapidly reacting Fmoc-Cl and much slower Fmoc-OSu were examined. The derivatization products were first analyzed by direct infusion MS and MS/MS. In the MS spectra of the IR1A isomer, a doubly derivatized peptide ($Fmoc_2$-IR1A) was observed after reaction with Fmoc-Cl (Figure 15). The same reaction of IR1B produced mainly a singly derivatized (Fmoc-IR1B) product. The MS/MS spectra of both derivatization products showed that the Fmoc-product was formed by reaction of an amino group close to the N-terminal end, whereas in the $Fmoc_2$-product another amino group close to the C-terminal end was also derivatized. The phosphorylation near the C-terminal end of IR1B most likely prevented reaction of the amino groups close to the C-terminal end and thus resulted in singly derivatized product in the rapid 10 min reaction. Based on these results, derivatization may enable separation of the isomers based on m/z ratio if the phosphorylation is close to the derivatized group and thus prevents the reaction. In turn, the slow derivatization by Fmoc-OSu resulted in $Fmoc_2$-products of both isomers.

The formation of different derivatization products may not be achieved in all cases, especially with more complicated samples, and it may also require a lot of optimization. Thus, the derivatization products were analyzed by MCE-ESI/MS. In addition to the $Fmoc_2$-IR1A product, a small peak of singly derivatized Fmoc-IR1A was observed after separation by MCE. However, even the reaction products Fmoc-IR1A and Fmoc-IR1B with the same m/z values could be separated by the MCE method (E = 150 V/cm) prior to MS analysis with migration times of 27.1 s (Fmoc-IR1A) and 34.6 s (Fmoc-IR1B). Similarly, the $Fmoc_2$-products formed in the reaction with Fmoc-OSu could be separated by the MCE method (E = 500 V/cm) with migration times of 27.4 s ($Fmoc_2$-IR1A) and 32.7 s ($Fmoc_2$-IR1B). The MCE separation also revealed Fmoc-IR1B product (t_{migr} = 27.0 s) formed in the reaction with Fmoc-OSu, that was detected only after separation from the $Fmoc_2$-IR1B product (t_{migr} = 32.7 s). The repeatability of migration times was good for all the reaction products (4.0–6.1% CV, n = 3, no IS). Overall, the developed method showed good performance in analysis of simple peptide samples. For further evaluation of the performance, the method should be applied to analysis of digested protein samples.

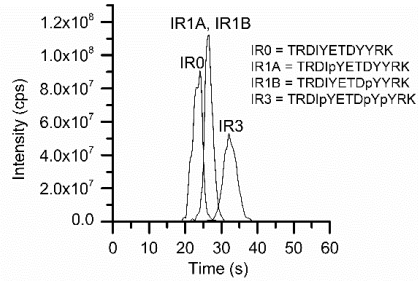

Figure 14 The extracted ion electropherograms of the most abundant $[M + 2H]^{2+}$ ions of the nonphosphorylated peptide (IR0), the monophosphorylated peptides (IR1A and IR1B), and the triply phosphorylated peptide (IR3), 50 µM each, separated by the optimized MCE-ESI/MS method. Reprinted with permission from ref. [172] originally published in Journal of Chromatography A.

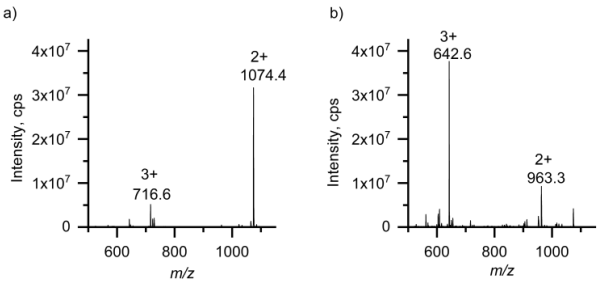

Figure 15 The MS spectra of derivatization products a) $Fmoc_2$-IR1A and b) Fmoc-IR1B from reaction with Fmoc-Cl. Adjusted with permission from ref. [172] originally published in Journal of Chromatography A.

5 SUMMARY AND CONCLUSIONS

In this thesis, the possibilities of microfluidic analytical devices in pharmaceutical research were demonstrated in selected applications with different analytical requirements. Special emphasis was put on requirements of drug metabolism studies and precision medicine.

One approach to more effective medication is targeted drug delivery with help of nanocarriers. In publication I, the risk of interactions between the PSi nanoformulations and CYP enzymes was demonstrated by study of enzyme kinetic parameters in pooled HLM. The highly polymorphic CYP2D6 was most affected by the studied nanoparticles with up to 60% loss of activity in the presence of TCPSi particles. The actual mechanisms, as well as the cellular uptake of the nanoparticles by hepatocytes have not been determined and should be investigated to understand the overall effects in vivo. The "assay cascade" for full characterization of nanomaterials developed by the European Nanomedicine Characterisation Laboratory (EUNCL) includes physical and chemical properties, as well as screening of immunological, hematological, and toxicological properties in vitro.[173] However, the effects on CYP metabolism are not included despite the critical role of these enzymes in metabolism of both drugs and other xenobiotics.

In addition to xenobiotics, also individual characteristics, including genetic polymorphism, age, sex, and disease, as well as other environmental factors, cause significant inter-individual variation in CYP activity. Taking these differences into account in selection of the most efficient and safe treatment for each patient individually, is important aspect of precision medicine. Genetic tests for most common polymorphic variants of *CYP2D6*, *CYP2C9*, and *CYP2C19* have been developed and commercialized.[10,42] However, these test do not recognize rare variants, and even more importantly, all the other factors affecting the CYP activities are not considered.

In publication II, a simple microfluidic platform (based on paper-like FCC coating) for screening of the individual differences in enzyme activities was developed and preliminarily characterized. A lot of further optimization and characterization is still required to improve sensitivity, accuracy, and precision of the personalized CYP screening. The basic idea of the platform was however demonstrated by analyzing CYP1A2 and CYP2A6 activities in liver microsomes from three individual donors. The amount of microsomes required for the analysis is very small and thus microsomes can be prepared of liver biopsy. Although liver biopsy is a medical procedure, that requires also trained personnel, and more invasive than a simple finger prick to obtain a drop of blood, the proposed approach does not require administration of a cocktail of probe drugs with high risk of adverse effects. The assay was also designed to be compatible with conventional well-plate reader and thus does not require any special instrumentation. The study of enzyme activities from liver

microsomes would most likely be best suited for situations where liver biopsy is relevant also for diagnosis etc. For example, the patients with hepatocellular carcinoma, the most common type of cancer in liver, suffer also from severe liver dysfunction, including changes in CYP metabolism.[174] Together with multiple medications for the cancer, the risk of adverse effects and toxicity related CYP metabolism can be highly increased.

Advanced miniaturized analytical separation systems, including microchip electrophoresis, enable analysis of more complex samples. MCE is a widely studied separation method, which benefits from miniaturization. The feasibility of a commercial MCE-EC device for CYP metabolism studies [152] and analysis of morphine from plasma and brain samples (III) was evaluated. The method developed for CYP metabolism studies showed good precision and LODs in low micromolar range. However, the sensitivity of the system was not sufficient for CYP metabolism studies with the probe reactions recommended by the FDA. Instead, the sensitivity of the system was found to be sufficient for analysis of morphine in biological matrices. A quantitative method, including off-chip LLE and on-chip electrokinetic stacking, was developed with good precision and accuracy. This kind of simple, small, and relatively cheap commercial device could be beneficial also in other laboratories than those focusing on analytical chemistry. It is especially suitable for targeted analysis of electroactive compounds and further improvements in automatization and integration of the sample handling would enhance the applicability of the system by also operators without special expertise in analytical chemistry. A targeted method could be used e.g., to provide chemical information in addition to behavioral monitoring in animal research facilities.

The capability of MCE was also demonstrated in a more challenging analytical task i.e., separation of phosphopeptides and especially the positional phosphorylation isomers (IV). MCE was combined to mass spectrometric detection via monolithically integrated ESI tip on the microchip. The developed method was able to separate nonphosphorylated insulin receptor peptide from the corresponding monophosphorylated and triply phosphorylated peptides with same amino acid sequence in less than 40 s. The monophosphorylated isomers with identical m/z ratio could not be separated in their native form and thus a derivatization protocol was applied. The rapid derivatization by Fmoc-Cl resulted in different reaction products, with different m/z values, of the two isomers enabling their separation by MS. Instead, the slow overnight derivatization by Fmoc-OSu, resulted mainly in the $Fmoc_2$-product of both monophosphorylated isomers. However, even the similar $Fmoc_2$-products with equal m/z values could be separated by MCE before the MS analysis. To demonstrate the suitability of the method, further studies with digested protein samples should be performed. The more complex samples, with a wide variety of different peptides, will challenge the method, especially considering the low abundance of the phosphopeptides. An additional (on-chip) phosphopeptide enrichment step might be necessary

before derivatization and separation of the positional phosphopeptide isomers.

In all, the work described in this thesis provides a glimpse into the possibilities of microfluidic analytical techniques in pharmaceutical research. The simplicity, speed, low costs, and parallelization makes these techniques highly interesting in a variety of applications. The envisioned use of the simplest equipment-free devices (including μPADs) for point-of-care diagnostics in the developing countries, can be one of the future applications of microfluidics. Still, need for fast and simple analytical techniques does exist also in the developed countries. For example, the increasing interest in precision medicine will require tools that enable identification of the individual characteristics that are considered to select the most safe and effective treatment for each patient. Miniaturized analytical techniques could be powerful also in these applications in the future. Microchip electrophoresis, the most commonly miniaturized separation technique, is not yet in a position where it would be widely applied in routine analysis. Especially, the robustness is often questioned. The MCE-EC method developed in this thesis demonstrated repeatable quantitative analysis, and more validated quantitative methods are needed to convince the possible users outside the "microfluidic community". Further advances in integration of additional steps on the same microchip and increase in the level of automatization will also enhance the way of MCE to routine use in pharmaceutical research.

REFERENCES

[1] A. Manz, N. Graber, H.M. Widmer, Miniaturized total chemical analysis systems: A novel concept for chemical sensing, Sens. Actuators B Chem. 1 (1990) 244–248. doi:10.1016/0925-4005(90)80209-I.

[2] P. Anzenbacher, E. Anzenbacherová, Cytochromes P450 and metabolism of xenobiotics, Cell. Mol. Life Sci. CMLS. 58 (2001) 737–747. doi:10.1007/PL00000897.

[3] U.M. Zanger, M. Schwab, Cytochrome P450 enzymes in drug metabolism: Regulation of gene expression, enzyme activities, and impact of genetic variation, Pharmacol. Ther. 138 (2013) 103–141. doi:10.1016/j.pharmthera.2012.12.007.

[4] W. Jung, J. Han, J.-W. Choi, C.H. Ahn, Point-of-care testing (POCT) diagnostic systems using microfluidic lab-on-a-chip technologies, Microelectron. Eng. 132 (2015) 46–57. doi:10.1016/j.mee.2014.09.024.

[5] National Research Council, Toward Precision Medicine: Building a Knowledge Network for Biomedical Research and a New Taxonomy of Disease, National Academies Press, Washington, D.C., 2011. doi:10.17226/13284.

[6] C. Fornaguera, M.J. García-Celma, Personalized Nanomedicine: A Revolution at the Nanoscale, J. Pers. Med. 7 (2017). doi:10.3390/jpm7040012.

[7] P.Y. Muller, M.N. Milton, The determination and interpretation of the therapeutic index in drug development, Nat. Rev. Drug Discov. 11 (2012) 751–761. doi:10.1038/nrd3801.

[8] Z. Zhang, W. Tang, Drug metabolism in drug discovery and development, Acta Pharm. Sin. B. 8 (2018) 721–732. doi:10.1016/j.apsb.2018.04.003.

[9] D.C. Evans, A.P. Watt, D.A. Nicoll-Griffith, T.A. Baillie, Drug–Protein Adducts: An Industry Perspective on Minimizing the Potential for Drug Bioactivation in Drug Discovery and Development, Chem. Res. Toxicol. 17 (2004) 3–16. doi:10.1021/tx034170b.

[10] P. Manikandan, S. Nagini, Cytochrome P450 Structure, Function and Clinical Significance: A Review, Curr. Drug Targets. 19 (2018) 38–54. doi:10.2174/1389450118666170125144557.

[11] S. Preissner, K. Kroll, M. Dunkel, C. Senger, G. Goldsobel, D. Kuzman, S. Guenther, R. Winnenburg, M. Schroeder, R. Preissner, SuperCYP: a comprehensive database on Cytochrome P450 enzymes including a tool for analysis of CYP-drug interactions, Nucleic Acids Res. 38 (2010) D237–D243. doi:10.1093/nar/gkp970.

[12] X. Pan, M. Ning, H. Jeong, Transcriptional Regulation of CYP2D6 Expression, Drug Metab. Dispos. 45 (2017) 42–48. doi:10.1124/dmd.116.072249.

[13] M. Ingelman-Sundberg, Pharmacogenetics of cytochrome P450 and its applications in drug therapy: the past, present and future, Trends Pharmacol. Sci. 25 (2004) 193–200. doi:10.1016/j.tips.2004.02.007.

[14] M. Ingelman-Sundberg, S.C. Sim, A. Gomez, C. Rodriguez-Antona, Influence of cytochrome P450 polymorphisms on drug therapies: Pharmacogenetic, pharmacoepigenetic and clinical aspects, Pharmacol. Ther. 116 (2007) 496–526. doi:10.1016/j.pharmthera.2007.09.004.

[15] Y. Zhou, M. Ingelman-Sundberg, V. Lauschke, Worldwide Distribution of Cytochrome P450 Alleles: A Meta-analysis of Population-scale Sequencing Projects, Clin. Pharmacol. Ther. 102 (2017) 688–700. doi:10.1002/cpt.690.

[16] C. Kawanishi, S. Lundgren, H. Ågren, L. Bertilsson, Increased incidence of CYP2D6 gene duplication in patients with persistent mood disorders: ultrarapid metabolism of antidepressants as a cause of nonresponse. A pilot study, Eur. J. Clin. Pharmacol. 59 (2004) 803–807. doi:10.1007/s00228-003-0701-4.
[17] U. Stamer, F. Stüber, T. Muders, F. Musshoff, Respiratory Depression with Tramadol in a Patient with Renal Impairment and CYP2D6 Gene Duplication, Anesth. Analg. 107 (2008) 926–929. doi:10.1213/ane.0b013e31817b796e.
[18] J. de Leon, M.T. Susce, R.-M. Pan, M. Fairchild, W.H. Koch, P.J. Wedlund, The CYP2D6 Poor Metabolizer Phenotype May Be Associated With Risperidone Adverse Drug Reactions and Discontinuation, J. Clin. Psychiatry. 66 (2005) 15–27.
[19] J.A. Johnson, L. Gong, M. Whirl-Carrillo, B.F. Gage, S.A. Scott, C.M. Stein, J.L. Anderson, S.E. Kimmel, M.T.M. Lee, M. Pirmohamed, M. Wadelius, T.E. Klein, R.B. Altman, Clinical Pharmacogenetics Implementation Consortium Guidelines for CYP2C9 and VKORC1 Genotypes and Warfarin Dosing, Clin. Pharmacol. Ther. 90 (2011) 625–629. doi:10.1038/clpt.2011.185.
[20] M. Nakajima, T. Fukami, H. Yamanaka, E. Higashi, H. Sakai, R. Yoshida, J.-T. Kwon, H.L. McLeod, T. Yokoi, Comprehensive evaluation of variability in nicotine metabolism and CYP2A6 polymorphic alleles in four ethnic populations, Clin. Pharmacol. Ther. 80 (2006) 282–297. doi:10.1016/j.clpt.2006.05.012.
[21] O. Soldin, D. Mattison, Sex Differences in Pharmacokinetics and Pharmacodynamics, Clin. Pharmacokinet. 48 (2009) 143–157. doi:10.2165/00003088-200948030-00001.
[22] M.M. Cotreau, L.L. von Moltke, D.D.J. Greenblatt, The Influence of Age and Sex on the Clearance of Cytochrome P450 3A Substrates, Clin. Pharmacokinet. 44 (2012) 33–60. doi:10.2165/00003088-200544010-00002.
[23] J.-A. Tanner, R.F. Tyndale, Variation in CYP2A6 Activity and Personalized Medicine, J. Pers. Med. 7 (2017). doi:10.3390/jpm7040018.
[24] R.H. Elbekai, H.M.K. and A.O.S. El-Kadi, The Effect of Liver Cirrhosis on the Regulation and Expression of Drug Metabolizing Enzymes, Curr. Drug Metab. 5 (2004) 157–167. doi:10.2174/1389200043489054.
[25] C.D. Fisher, A.J. Lickteig, L.M. Augustine, J. Ranger-Moore, J.P. Jackson, S.S. Ferguson, N.J. Cherrington, Hepatic Cytochrome P450 Enzyme Alterations in Humans with Progressive Stages of Nonalcoholic Fatty Liver Disease, Drug Metab. Dispos. 37 (2009) 2087–2094. doi:10.1124/dmd.109.027466.
[26] J.-P. Villeneuve, V. Pichette, Cytochrome P450 and Liver Diseases, Curr. Drug Metab. 5 (2004) 273–282. doi:10.2174/1389200043335531.
[27] K.A. Slaviero, S.J. Clarke, L.P. Rivory, Inflammatory response: an unrecognised source of variability in the pharmacokinetics and pharmacodynamics of cancer chemotherapy, Lancet Oncol. 4 (2003) 224–232. doi:10.1016/S1470-2045(03)01034-9.
[28] A.E. Aitken, T.A. Richardson, E.T. Morgan, Regulation of Drug-Metabolizing Enzymes and Transporters in Inflammation, Annu. Rev. Pharmacol. Toxicol. 46 (2006) 123–149. doi:10.1146/annurev.pharmtox.46.120604.141059.
[29] V. Tomankova, P. Anzenbacher, E. Anzenbacherova, Effects of obesity on liver cytochromes P450 in various animal models, Biomed. Pap. 161 (2017) 144–151. doi:10.5507/bp.2017.026.
[30] L.M. Tompkins, A.D. Wallace, Mechanisms of cytochrome P450 induction, J. Biochem. Mol. Toxicol. 21 (2007) 176–181. doi:10.1002/jbt.20180.

[31] O. Pelkonen, M. Turpeinen, J. Hakkola, P. Honkakoski, J. Hukkanen, H. Raunio, Inhibition and induction of human cytochrome P450 enzymes: current status, Arch. Toxicol. 82 (2008) 667–715. doi:10.1007/s00204-008-0332-8.
[32] E. Fontana, P.M. Dansette, S.M. Poli, Cytochrome P450 Enzymes Mechanism Based Inhibitors: Common Sub-Structures and Reactivity, Curr. Drug Metab. 6 (2005) 413–451. doi:10.2174/138920005774330639.
[33] M.J. Hanley, P. Cancalon, W.W. Widmer, D.J. Greenblatt, The effect of grapefruit juice on drug disposition, Expert Opin. Drug Metab. Toxicol. 7 (2011) 267–286. doi:10.1517/17425255.2011.553189.
[34] J.M. MacDougall, K. Fandrick, X. Zhang, S.V. Serafin, J.R. Cashman, Inhibition of Human Liver Microsomal (S)-Nicotine Oxidation by (–)-Menthol and Analogues, Chem. Res. Toxicol. 16 (2003) 988–993. doi:10.1021/tx0340551.
[35] N.L. Benowitz, B. Herrera, P. Jacob, Mentholated Cigarette Smoking Inhibits Nicotine Metabolism, J. Pharmacol. Exp. Ther. 310 (2004) 1208–1215. doi:10.1124/jpet.104.066902.
[36] K. Abass, O. Pelkonen, The inhibition of major human hepatic cytochrome P450 enzymes by 18 pesticides: Comparison of the N-in-one and single substrate approaches, Toxicol. In Vitro. 27 (2013) 1584–1588. doi:10.1016/j.tiv.2012.05.003.
[37] H. Ozaki, K. Sugihara, Y. Watanabe, S. Ohta, S. Kitamura, Cytochrome P450-inhibitory activity of parabens and phthalates used in consumer products, J. Toxicol. Sci. 41 (2016) 551–560. doi:10.2131/jts.41.551.
[38] K. Jonsson-Schmunk, S.C. Schafer, M.A. Croyle, Impact of nanomedicine on hepatic cytochrome P450 3A4 activity: things to consider during pre-clinical and clinical studies, J. Pharm. Investig. 48 (2018) 113–134. doi:10.1007/s40005-017-0376-y.
[39] M. Bar-Zeev, Y.D. Livney, Y.G. Assaraf, Targeted nanomedicine for cancer therapeutics: Towards precision medicine overcoming drug resistance, Drug Resist. Updat. 31 (2017) 15–30. doi:10.1016/j.drup.2017.05.002.
[40] FDA Website - Table of Pharmacogenomic Biomarkers in Drug Labeling, FDA. (2019). https://www.fda.gov/drugs/science-research-drugs/table-pharmacogenomic-biomarkers-drug-labeling (accessed May 14, 2019).
[41] L. Dean, Warfarin Therapy and VKORC1 and CYP Genotype, in: V. Pratt, H. McLeod, W. Rubinstein, L. Dean, B. Kattman, A. Malheiro (Eds.), Med. Genet. Summ., National Center for Biotechnology Information (US), Bethesda (MD), 2012. http://www.ncbi.nlm.nih.gov/books/NBK84174/ (accessed May 7, 2019).
[42] C.F. Samer, K.I. Lorenzini, V. Rollason, Y. Daali, J.A. Desmeules, Applications of CYP450 Testing in the Clinical Setting, Mol. Diagn. Ther. 17 (2013) 165–184. doi:10.1007/s40291-013-0028-5.
[43] Y. Daali, C. Samer, J. Déglon, A. Thomas, J. Chabert, M. Rebsamen, C. Staub, P. Dayer, J. Desmeules, Oral flurbiprofen metabolic ratio assessment using a single-point dried blood spot, Clin. Pharmacol. Ther. 91 (2012) 489–496. doi:10.1038/clpt.2011.247.
[44] S.C. Terry, J.H. Jerman, J.B. Angell, A gas chromatographic air analyzer fabricated on a silicon wafer, IEEE Trans. Electron Devices. 26 (1979) 1880–1886. doi:10.1109/T-ED.1979.19791.
[45] E.R. Castro, A. Manz, Present state of microchip electrophoresis: State of the art and routine applications, J. Chromatogr. A. 1382 (2015) 66–85. doi:10.1016/j.chroma.2014.11.034.
[46] N. Nordman, S. Laurén, T. Kotiaho, S. Franssila, R. Kostiainen, T. Sikanen, Interfacing microchip isoelectric focusing with on-chip electrospray ionization mass spectrometry, J. Chromatogr. A. 1398 (2015) 121–126. doi:10.1016/j.chroma.2015.04.031.

[47] J. Wen, Y. Lin, F. Xiang, D.W. Matson, H.R. Udseth, R.D. Smith, Microfabricated isoelectric focusing device for direct electrospray ionization-mass spectrometry, Electrophoresis. 21 (2000) 191–197. doi:10.1002/(SICI)1522-2683(20000101)21:1<191::AID-ELPS191>3.0.CO;2-M.
[48] L. Chen, J. E. Prest, P. R. Fielden, N. J. Goddard, A. Manz, P.J. R. Day, Miniaturised isotachophoresis analysis, Lab. Chip. 6 (2006) 474–487. doi:10.1039/B515551G.
[49] Y. Du, E. Wang, Separation and Detection of Narcotic Drugs on a Microchip Using Micellar Electrokinetic Chromatography and Electrochemiluminescence, Electroanalysis. 20 (2008) 643–647. doi:10.1002/elan.200704117.
[50] Y. Ding, Y. Qi, X. Suo, Rapid determination of β2-agonists in urine samples by microchip micellar electrokinetic chromatography with pulsed electrochemical detection, Anal. Methods. 5 (2013) 2623–2629. doi:10.1039/C3AY00061C.
[51] G. Zhang, C. Qian, Y. Xu, X. Feng, W. Du, B.-F. Liu, Open tubular CEC in a microfluidic chip for rapid chiral recognition, J. Sep. Sci. 32 (2009) 374–380. doi:10.1002/jssc.200800507.
[52] S. Shen, Y. Li, S. Wakida, Characterization of dissolved organic carbon at low levels in environmental waters by microfluidic-chip-based capillary gel electrophoresis with a laser-induced fluorescence detector, Environ. Monit. Assess. 166 (2010) 573–580. doi:10.1007/s10661-009-1024-4.
[53] C. Wenz, M. Marchetti-Deschmann, E. Herwig, E. Schröttner, G. Allmaier, L. Trojer, M. Vollmer, A. Rüfer, A fluorescent derivatization method of proteins for the detection of low-level impurities by microchip capillary gel electrophoresis, Electrophoresis. 31 (2010) 611–617. doi:10.1002/elps.200900346.
[54] J.M. Karlinsey, Sample introduction techniques for microchip electrophoresis: A review, Anal. Chim. Acta. 725 (2012) 1–13. doi:10.1016/j.aca.2012.02.052.
[55] S.C. Jacobson, Roland. Hergenroder, L.B. Koutny, R.J. Warmack, J.Michael. Ramsey, Effects of Injection Schemes and Column Geometry on the Performance of Microchip Electrophoresis Devices, Anal. Chem. 66 (1994) 1107–1113. doi:10.1021/ac00079a028.
[56] P.N. Nge, C.I. Rogers, A.T. Woolley, Advances in Microfluidic Materials, Functions, Integration, and Applications, Chem. Rev. 113 (2013) 2550–2583. doi:10.1021/cr300337x.
[57] C. Iliescu, H. Taylor, M. Avram, J. Miao, S. Franssila, A practical guide for the fabrication of microfluidic devices using glass and silicon, Biomicrofluidics. 6 (2012) 16505–1650516. doi:10.1063/1.3689939.
[58] H. Becker, C. Gärtner, Polymer microfabrication technologies for microfluidic systems, Anal. Bioanal. Chem. 390 (2008) 89–111. doi:10.1007/s00216-007-1692-2.
[59] D.C. Duffy, J.C. McDonald, O.J.A. Schueller, G.M. Whitesides, Rapid Prototyping of Microfluidic Systems in Poly(dimethylsiloxane), Anal. Chem. 70 (1998) 4974–4984. doi:10.1021/ac980656z.
[60] W. Yang, X. Sun, H.-Y. Wang, A.T. Woolley, Integrated Microfluidic Device for Serum Biomarker Quantitation Using Either Standard Addition or a Calibration Curve, Anal. Chem. 81 (2009) 8230–8235. doi:10.1021/ac901566s.
[61] Y. Wang, H. Chen, Q. He, S.A. Soper, A high-performance polycarbonate electrophoresis microchip with integrated three-electrode system for end-channel amperometric detection, Electrophoresis. 29 (2008) 1881–1888. doi:10.1002/elps.200700377.

[62] T. Sikanen, L. Heikkilä, S. Tuomikoski, R.A. Ketola, R. Kostiainen, S. Franssila, T. Kotiaho, Performance of SU-8 Microchips as Separation Devices and Comparison with Glass Microchips, Anal. Chem. 79 (2007) 6255–6263. doi:10.1021/ac0703956.
[63] S.M. Tähkä, A. Bonabi, M.-E. Nordberg, M. Kanerva, Ville.P. Jokinen, T.M. Sikanen, Thiol-ene microfluidic devices for microchip electrophoresis: Effects of curing conditions and monomer composition on surface properties, J. Chromatogr. A. 1426 (2015) 233–240. doi:10.1016/j.chroma.2015.11.072.
[64] S.M. Tähkä, A. Bonabi, V.P. Jokinen, T.M. Sikanen, Aqueous and non-aqueous microchip electrophoresis with on-chip electrospray ionization mass spectrometry on replica-molded thiol-ene microfluidic devices, J. Chromatogr. A. 1496 (2017) 150–156. doi:10.1016/j.chroma.2017.03.018.
[65] A. Manz, D.J. Harrison, E.M.J. Verpoorte, James.C. Fettinger, A. Paulus, H. Lüdi, H.M. Widmer, Planar chips technology for miniaturization and integration of separation techniques into monitoring systems: Capillary electrophoresis on a chip, J. Chromatogr. A. 593 (1992) 253–258. doi:10.1016/0021-9673(92)80293-4.
[66] D.Jed. Harrison, Andreas. Manz, Zhonghui. Fan, Hans. Luedi, H.Michael. Widmer, Capillary electrophoresis and sample injection systems integrated on a planar glass chip, Anal. Chem. 64 (1992) 1926–1932. doi:10.1021/ac00041a030.
[67] S.C. Jacobson, Roland. Hergenroder, L.B. Koutny, J.Michael. Ramsey, High-Speed Separations on a Microchip, Anal. Chem. 66 (1994) 1114–1118. doi:10.1021/ac00079a029.
[68] D.E.W. Patabadige, S. Jia, J. Sibbitts, J. Sadeghi, K. Sellens, C.T. Culbertson, Micro Total Analysis Systems: Fundamental Advances and Applications, Anal. Chem. 88 (2016) 320–338. doi:10.1021/acs.analchem.5b04310.
[69] F. Yang, X. Li, W. Zhang, J. Pan, Z. Chen, A facile light-emitting-diode induced fluorescence detector coupled to an integrated microfluidic device for microchip electrophoresis, Talanta. 84 (2011) 1099–1106. doi:10.1016/j.talanta.2011.03.020.
[70] S. Wang, X. Li, J. Yang, X. Yang, F. Hou, Z. Chen, Rapid Determination of Creatinine in Human Urine by Microchip Electrophoresis with LED Induced Fluorescence Detection, Chromatographia. 75 (2012) 1287–1293. doi:10.1007/s10337-012-2324-3.
[71] B. Zhang, Z. Chen, Y. Yu, J. Yang, J. Pan, Determination of Sulfonamides in Pharmaceuticals and Rabbit Plasma by Microchip Electrophoresis with LED-IF Detection, Chromatographia. 76 (2013) 821–829. doi:10.1007/s10337-013-2479-6.
[72] M.A. Schwarz, P.C. Hauser, Recent developments in detection methods for microfabricated analytical devices, Lab. Chip. 1 (2001) 1–6. doi:10.1039/B103795C.
[73] P.D. Ohlsson, O. Ordeig, K.B. Mogensen, J.P. Kutter, Electrophoresis microchip with integrated waveguides for simultaneous native UV fluorescence and absorbance detection, Electrophoresis. 30 (2009) 4172–4178. doi:10.1002/elps.200900393.
[74] K.W. Ro, K. Lim, B.C. Shim, J.H. Hahn, Integrated Light Collimating System for Extended Optical-Path-Length Absorbance Detection in Microchip-Based Capillary Electrophoresis, Anal. Chem. 77 (2005) 5160–5166. doi:10.1021/ac050420c.
[75] S. Götz, U. Karst, Recent developments in optical detection methods for microchip separations, Anal. Bioanal. Chem. 387 (2007) 183–192. doi:10.1007/s00216-006-0820-8.
[76] M.H. Ghanim, M.Z. Abdullah, Integrating amperometric detection with electrophoresis microchip devices for biochemical assays: Recent developments, Talanta. 85 (2011) 28–34. doi:10.1016/j.talanta.2011.04.069.

[77] W.R. Vandaveer, S.A. Pasas-Farmer, D.J. Fischer, C.N. Frankenfeld, S.M. Lunte, Recent developments in electrochemical detection for microchip capillary electrophoresis, Electrophoresis. 25 (2004) 3528–3549. doi:10.1002/elps.200406115.
[78] E. Verpoorte, Chip vision - optics for microchips, Lab. Chip. 3 (2003) 42N-52N. doi:10.1039/B307927A.
[79] T. Sikanen, S. Franssila, T.J. Kauppila, R. Kostiainen, T. Kotiaho, R.A. Ketola, Microchip technology in mass spectrometry, Mass Spectrom. Rev. 29 (2010) 351–391. doi:10.1002/mas.20238.
[80] R.S. Ramsey, J.M. Ramsey, Generating Electrospray from Microchip Devices Using Electroosmotic Pumping, Anal. Chem. 69 (1997) 1174–1178. doi:10.1021/ac9610671.
[81] Q. Xue, F. Foret, Y.M. Dunayevskiy, P.M. Zavracky, N.E. McGruer, B.L. Karger, Multichannel Microchip Electrospray Mass Spectrometry, Anal. Chem. 69 (1997) 426–430. doi:10.1021/ac9607119.
[82] J. Kameoka, H.G. Craighead, H. Zhang, J. Henion, A Polymeric Microfluidic Chip for CE/MS Determination of Small Molecules, Anal. Chem. 73 (2001) 1935–1941. doi:10.1021/ac001533t.
[83] J. Li, C. Wang, J.F. Kelly, D.J. Harrison, P. Thibault, Rapid and sensitive separation of trace level protein digests using microfabricated devices coupled to a quadrupole - time-of-flight mass spectrometer, Electrophoresis. 21 (2000) 198–210. doi:10.1002/(SICI)1522-2683(20000101)21:1<198::AID-ELPS198>3.0.CO;2-V.
[84] B. Zhang, H. Liu, B.L. Karger, F. Foret, Microfabricated Devices for Capillary Electrophoresis–Electrospray Mass Spectrometry, Anal. Chem. 71 (1999) 3258–3264. doi:10.1021/ac990090u.
[85] T. Sikanen, S. Tuomikoski, R.A. Ketola, R. Kostiainen, S. Franssila, T. Kotiaho, Fully Microfabricated and Integrated SU-8-Based Capillary Electrophoresis-Electrospray Ionization Microchips for Mass Spectrometry, Anal. Chem. 79 (2007) 9135–9144. doi:10.1021/ac071531+.
[86] D.T. Snyder, C.J. Pulliam, Z. Ouyang, R.G. Cooks, Miniature and Fieldable Mass Spectrometers: Recent Advances, Anal. Chem. 88 (2016) 2–29. doi:10.1021/acs.analchem.5b03070.
[87] N. Nuchtavorn, W. Suntornsuk, S.M. Lunte, L. Suntornsuk, Recent applications of microchip electrophoresis to biomedical analysis, J. Pharm. Biomed. Anal. 113 (2015) 72–96. doi:10.1016/j.jpba.2015.03.002.
[88] FDA, U.S. Food and Drug Administration, Guidance for Industry – Bioanalytical Method Validation, (2018).
[89] International Conference on Harmonisation of Technical Requirements for Registration of Pharmaceuticals for Human Use (ICH), Validation of Analytical Procedures: Text and Methodology Q2(R1), (1994). http://www.ich.org/products/guidelines/quality/quality-single/article/validation-of-analytical-procedures-text-and-methodology.html (accessed June 26, 2017).
[90] K. Tolba, D. Belder, Fast quantitative determination of diuretic drugs in tablets and human urine by microchip electrophoresis with native fluorescence detection, Electrophoresis. 28 (2007) 2934–2941. doi:10.1002/elps.200600520.
[91] N. Nordman, B. Barrios-Lopez, S. Laurén, P. Suvanto, T. Kotiaho, S. Franssila, R. Kostiainen, T. Sikanen, Shape-anchored porous polymer monoliths for integrated online solid-phase extraction-microchip electrophoresis-electrospray ionization mass spectrometry, Electrophoresis. 36 (2015) 428–432. doi:10.1002/elps.201400278.
[92] Y.H. Tennico, V.T. Remcho, In-line extraction employing functionalized magnetic particles for capillary and microchip electrophoresis, Electrophoresis. 31 (2010) 2548–2557. doi:10.1002/elps.201000256.

[93] C. Wang, A.B. Jemere, D.J. Harrison, Multifunctional protein processing chip with integrated digestion, solid-phase extraction, separation and electrospray, Electrophoresis. 31 (2010) 3703–3710. doi:10.1002/elps.201000317.
[94] A. Jönsson, J. P. Lafleur, D. Sticker, J. P. Kutter, An all thiol–ene microchip for solid phase extraction featuring an in situ polymerized monolith and integrated 3D replica-molded emitter for direct electrospray mass spectrometry, Anal. Methods. 10 (2018) 2854–2862. doi:10.1039/C8AY00646F.
[95] V. Sahore, M. Sonker, A.V. Nielsen, R. Knob, S. Kumar, A.T. Woolley, Automated microfluidic devices integrating solid-phase extraction, fluorescent labeling, and microchip electrophoresis for preterm birth biomarker analysis, Anal. Bioanal. Chem. 410 (2018) 933–941. doi:10.1007/s00216-017-0548-7.
[96] N. Nordman, T. Sikanen, M.-E. Moilanen, S. Aura, T. Kotiaho, S. Franssila, R. Kostiainen, Rapid and sensitive drug metabolism studies by SU-8 microchip capillary electrophoresis-electrospray ionization mass spectrometry, J. Chromatogr. A. 1218 (2011) 739–745. doi:10.1016/j.chroma.2010.12.010.
[97] T. Sikanen, S. Pedersen-Bjergaard, H. Jensen, R. Kostiainen, K.E. Rasmussen, T. Kotiaho, Implementation of droplet-membrane-droplet liquid-phase microextraction under stagnant conditions for lab-on-a-chip applications, Anal. Chim. Acta. 658 (2010) 133–140. doi:10.1016/j.aca.2009.11.002.
[98] Y.A. Asl, Y. Yamini, S. Seidi, M. Rezazadeh, Simultaneous extraction of acidic and basic drugs via on-chip electromembrane extraction, Anal. Chim. Acta. 937 (2016) 61–68. doi:10.1016/j.aca.2016.07.048.
[99] F. Zarghampour, Y. Yamini, M. Baharfar, M. Faraji, Simultaneous extraction of acidic and basic drugs via on-chip electromembrane extraction using a single-compartment microfluidic device, Analyst. 144 (2019) 1159–1166. doi:10.1039/C8AN01668B.
[100] Y. Huang, S. Zhao, M. Shi, H. Liang, A microchip electrophoresis strategy with online labeling and chemiluminescence detection for simultaneous quantification of thiol drugs, J. Pharm. Biomed. Anal. 55 (2011) 889–894. doi:10.1016/j.jpba.2011.03.007.
[101] A. Fernández-la-Villa, D.F. Pozo-Ayuso, M. Castaño-Álvarez, New analytical portable instrument for microchip electrophoresis with electrochemical detection, Electrophoresis. 31 (2010) 2641–2649. doi:10.1002/elps.201000100.
[102] X. Li, J. Pan, F. Yang, J. Feng, J. Mo, Z. Chen, Simple amperometric detector for microchip capillary electrophoresis, and its application to the analysis of dopamine and catechol, Microchim. Acta. 174 (2011) 123. doi:10.1007/s00604-011-0592-5.
[103] Q.-L. Zhang, J.-J. Xu, X.-Y. Li, H.-Z. Lian, H.-Y. Chen, Determination of morphine and codeine in urine using poly(dimethylsiloxane) microchip electrophoresis with electrochemical detection, J. Pharm. Biomed. Anal. 43 (2007) 237–242. doi:10.1016/j.jpba.2006.06.003.
[104] A. Fernández-la-Villa, V. Bertrand-Serrador, D.F. Pozo-Ayuso, M. Castaño-Álvarez, Fast and reliable urine analysis using a portable platform based on microfluidic electrophoresis chips with electrochemical detection, Anal. Methods. 5 (2013) 1494–1501. doi:10.1039/C2AY26166A.
[105] Q.-L. Zhang, H.-Z. Lian, W.-H. Wang, H.-Y. Chen, Separation of caffeine and theophylline in poly(dimethylsiloxane) microchannel electrophoresis with electrochemical detection, J. Chromatogr. A. 1098 (2005) 172–176. doi:10.1016/j.chroma.2005.08.055.

[106] F. Schwarzkopf, T. Scholl, S. Ohla, D. Belder, Improving sensitivity in microchip electrophoresis coupled to ESI-MS/MS on the example of a cardiac drug mixture, Electrophoresis. 35 (2014) 1880–1886. doi:10.1002/elps.201300615.
[107] A. Lloyd, M. Russell, L. Blanes, P. Doble, C. Roux, Lab-on-a-chip screening of methamphetamine and pseudoephedrine in samples from clandestine laboratories, Forensic Sci. Int. 228 (2013) 8–14. doi:10.1016/j.forsciint.2013.01.036.
[108] A. Lloyd, M. Russell, L. Blanes, R. Somerville, P. Doble, C. Roux, The application of portable microchip electrophoresis for the screening and comparative analysis of synthetic cathinone seizures, Forensic Sci. Int. 242 (2014) 16–23. doi:10.1016/j.forsciint.2014.06.013.
[109] G. Desmet, S. Eeltink, Fundamentals for LC Miniaturization, Anal. Chem. 85 (2013) 543–556. doi:10.1021/ac303317c.
[110] S. Thurmann, L. Mauritz, C. Heck, D. Belder, High-performance liquid chromatography on glass chips using precisely defined porous polymer monoliths as particle retaining elements, J. Chromatogr. A. 1370 (2014) 33–39. doi:10.1016/j.chroma.2014.10.008.
[111] K.M. Robotti, H. Yin, R. Brennen, L. Trojer, K. Killeen, Microfluidic HPLC-Chip devices with integral channels containing methylstyrenic-based monolithic media, J. Sep. Sci. 32 (2009) 3379–3387. doi:10.1002/jssc.200900379.
[112] P.A. Levkin, S. Eeltink, T.R. Stratton, R. Brennen, K. Robotti, H. Yin, K. Killeen, F. Svec, J.M.J. Fréchet, Monolithic porous polymer stationary phases in polyimide chips for the fast high-performance liquid chromatography separation of proteins and peptides, J. Chromatogr. A. 1200 (2008) 55–61. doi:10.1016/j.chroma.2008.03.025.
[113] L. Sainiemi, T. Nissilä, R. Kostiainen, S. Franssila, R.A. Ketola, A microfabricated micropillar liquid chromatographic chip monolithically integrated with an electrospray ionization tip, Lab. Chip. 12 (2011) 325–332. doi:10.1039/C1LC20874H.
[114] W. De Malsche, H. Eghbali, D. Clicq, J. Vangelooven, H. Gardeniers, G. Desmet, Pressure-Driven Reverse-Phase Liquid Chromatography Separations in Ordered Nonporous Pillar Array Columns, Anal. Chem. 79 (2007) 5915–5926. doi:10.1021/ac070352p.
[115] X. Yuan, R.D. Oleschuk, Advances in Microchip Liquid Chromatography, Anal. Chem. 90 (2018) 283–301. doi:10.1021/acs.analchem.7b04329.
[116] X. Wang, S. Wang, B. Gendhar, C. Cheng, C.K. Byun, G. Li, M. Zhao, S. Liu, Electroosmotic pumps for microflow analysis, Trends Anal. Chem. TRAC. 28 (2009) 64–74. doi:10.1016/j.trac.2008.09.014.
[117] W. Wang, C. Gu, K.B. Lynch, J.J. Lu, Z. Zhang, Q. Pu, S. Liu, High-Pressure Open-Channel On-Chip Electroosmotic Pump for Nanoflow High Performance Liquid Chromatography, Anal. Chem. 86 (2014) 1958–1964. doi:10.1021/ac4040345.
[118] L. Xia, C. Choi, S.C. Kothekar, D. Dutta, On-Chip Pressure Generation for Driving Liquid Phase Separations in Nanochannels, Anal. Chem. 88 (2016) 781–788. doi:10.1021/acs.analchem.5b03125.
[119] S.-H. Chiu, C.-H. Liu, An air-bubble-actuated micropump for on-chip blood transportation, Lab. Chip. 9 (2009) 1524–1533. doi:10.1039/b900139e.
[120] J. Nestler, A. Morschhauser, K. Hiller, T. Otto, S. Bigot, J. Auerswald, H.F. Knapp, J. Gavillet, T. Gessner, Polymer lab-on-chip systems with integrated electrochemical pumps suitable for large-scale fabrication, Int. J. Adv. Manuf. Technol. 47 (2010) 137–145. doi:10.1007/s00170-009-1948-4.

[121] P.Z. Kazemi, P.R. Selvaganapathy, C.Y. Ching, Electrohydrodynamic micropumps with asymmetric electrode geometries for microscale electronics cooling, IEEE Trans. Dielectr. Electr. Insul. 16 (2009) 483–488. doi:10.1109/TDEI.2009.4815182.
[122] A.V. Lemoff, A.P. Lee, An AC magnetohydrodynamic micropump, Sens. Actuators B Chem. 63 (2000) 178–185. doi:10.1016/S0925-4005(00)00355-5.
[123] S. Qian, H.H. Bau, Magneto-Hydrodynamics Based Microfluidics, Mech. Res. Commun. 36 (2009) 10–21. doi:10.1016/j.mechrescom.2008.06.013.
[124] J. Šesták, D. Moravcová, V. Kahle, Instrument platforms for nano liquid chromatography, J. Chromatogr. A. 1421 (2015) 2–17. doi:10.1016/j.chroma.2015.07.090.
[125] C.E.D. Nazario, M.R. Silva, M.S. Franco, F.M. Lanças, Evolution in miniaturized column liquid chromatography instrumentation and applications: An overview, J. Chromatogr. A. 1421 (2015) 18–37. doi:10.1016/j.chroma.2015.08.051.
[126] Agilent HPLC-Chip/MS System. https://www.agilent.com/en-us/products/liquid-chromatography/low-flow-lc-systems/1260-infinity-hplc-chip-ms-system/gp38314 (accessed April 23, 2019).
[127] Advion TriVersa NanoMate®. https://advion.com/products/triversa-nanomate/ (accessed April 20, 2019).
[128] Waters ionKey/MS - microflow UPLC Seperation with iKey. http://www.waters.com/waters/en_US/ionKey-MS---microflow-UPLC-Seperation-with-iKey/nav.htm?cid=134782630&locale=en_US (accessed April 20, 2019).
[129] New Objective PicoChip Innovation in High-Performance LC-MS. http://www.newobjective.com/products/columns/pch-2.shtml (accessed April 20, 2019).
[130] K.Y. Zhu, K.W. Leung, A.K.L. Ting, Z.C.F. Wong, W.Y.Y. Ng, R.C.Y. Choi, T.T.X. Dong, T. Wang, D.T.W. Lau, K.W.K. Tsim, Microfluidic chip based nano liquid chromatography coupled to tandem mass spectrometry for the determination of abused drugs and metabolites in human hair, Anal. Bioanal. Chem. 402 (2012) 2805–2815. doi:10.1007/s00216-012-5711-6.
[131] V. Houbart, A.-C. Servais, T.D. Charlier, J.L. Pawluski, F. Abts, M. Fillet, A validated microfluidics-based LC-chip-MS/MS method for the quantitation of fluoxetine and norfluoxetine in rat serum, Electrophoresis. 33 (2012) 3370–3379. doi:10.1002/elps.201200168.
[132] Martinez Andres W., Phillips Scott T., Butte Manish J., Whitesides George M., Patterned Paper as a Platform for Inexpensive, Low-Volume, Portable Bioassays, Angew. Chem. Int. Ed. 46 (2007) 1318–1320. doi:10.1002/anie.200603817.
[133] M. Santhiago, E.W. Nery, G.P. Santos, L.T. Kubota, Microfluidic paper-based devices for bioanalytical applications, Bioanalysis. 6 (2013) 89–106. doi:10.4155/bio.13.296.
[134] D.M. Cate, J.A. Adkins, J. Mettakoonpitak, C.S. Henry, Recent Developments in Paper-Based Microfluidic Devices, Anal. Chem. 87 (2015) 19–41. doi:10.1021/ac503968p.
[135] Y. Yang, E. Noviana, M.P. Nguyen, B.J. Geiss, D.S. Dandy, C.S. Henry, Paper-Based Microfluidic Devices: Emerging Themes and Applications, Anal. Chem. 89 (2017) 71–91. doi:10.1021/acs.analchem.6b04581.
[136] M.M. Gong, D. Sinton, Turning the Page: Advancing Paper-Based Microfluidics for Broad Diagnostic Application, Chem. Rev. 117 (2017) 8447–8480. doi:10.1021/acs.chemrev.7b00024.
[137] Y. Xia, J. Si, Z. Li, Fabrication techniques for microfluidic paper-based analytical devices and their applications for biological testing: A review, Biosens. Bioelectron. 77 (2016) 774–789. doi:10.1016/j.bios.2015.10.032.

[138] E.W. Nery, L.T. Kubota, Sensing approaches on paper-based devices: a review, Anal. Bioanal. Chem. 405 (2013) 7573–7595. doi:10.1007/s00216-013-6911-4.
[139] A.W. Martinez, S.T. Phillips, E. Carrilho, S.W. Thomas, H. Sindi, G.M. Whitesides, Simple Telemedicine for Developing Regions: Camera Phones and Paper-Based Microfluidic Devices for Real-Time, Off-Site Diagnosis, Anal. Chem. 80 (2008) 3699–3707. doi:10.1021/ac800112r.
[140] J. Adkins, K. Boehle, C. Henry, Electrochemical paper-based microfluidic devices, Electrophoresis. 36 (2015) 1811–1824. doi:10.1002/elps.201500084.
[141] N. Sharma, T. Barstis, B. Giri, Advances in paper-analytical methods for pharmaceutical analysis, Eur. J. Pharm. Sci. 111 (2018) 46–56. doi:10.1016/j.ejps.2017.09.031.
[142] G. Musile, L. Wang, J. Bottoms, F. Tagliaro, B. McCord, The development of paper microfluidic devices for presumptive drug detection, Anal. Methods. 7 (2015) 8025–8033. doi:10.1039/C5AY01432H.
[143] C.-A. Chen, P.-W. Wang, Y.-C. Yen, H.-L. Lin, Y.-C. Fan, S.-M. Wu, C.-F. Chen, Fast analysis of ketamine using a colorimetric immunosorbent assay on a paper-based analytical device, Sens. Actuators B Chem. 282 (2019) 251–258. doi:10.1016/j.snb.2018.11.071.
[144] A.A. Weaver, H. Reiser, T. Barstis, M. Benvenuti, D. Ghosh, M. Hunckler, B. Joy, L. Koenig, K. Raddell, M. Lieberman, Paper Analytical Devices for Fast Field Screening of Beta Lactam Antibiotics and Antituberculosis Pharmaceuticals, Anal. Chem. 85 (2013) 6453–6460. doi:10.1021/ac400989p.
[145] K.E. Boehle, C.S. Carrell, J. Caraway, C.S. Henry, Paper-Based Enzyme Competition Assay for Detecting Falsified β-Lactam Antibiotics, ACS Sens. 3 (2018) 1299–1307. doi:10.1021/acssensors.8b00163.
[146] A.A. Weaver, M. Lieberman, Paper Test Cards for Presumptive Testing of Very Low Quality Antimalarial Medications, Am. J. Trop. Med. Hyg. 92 (2015) 17–23. doi:10.4269/ajtmh.14-0384.
[147] M.T. Koesdjojo, Y. Wu, A. Boonloed, E.M. Dunfield, V.T. Remcho, Low-cost, high-speed identification of counterfeit antimalarial drugs on paper, Talanta. 130 (2014) 122–127. doi:10.1016/j.talanta.2014.05.050.
[148] FDA Website on Drug Development and Drug Interactions. http://www.fda.gov/Drugs/DevelopmentApprovalProcess/DevelopmentResources/DrugInteractionsLabeling/ucm093664.htm#inVitro (accessed June 7, 2016).
[149] R. Gottardo, A. Polettini, D. Sorio, J.P. Pascali, F. Bortolotti, E. Liotta, F. Tagliaro, Capillary zone electrophoresis (CZE) coupled to time-of-flight mass spectrometry (TOF-MS) applied to the analysis of illicit and controlled drugs in blood, Electrophoresis. 29 (2008) 4078–4087. doi:10.1002/elps.200800087.
[150] E. Jutila, R. Koivunen, I. Kiiski, R. Bollström, T. Sikanen, P. Gane, Microfluidic Lateral Flow Cytochrome P450 Assay on a Novel Printed Functionalized Calcium Carbonate-Based Platform for Rapid Screening of Human Xenobiotic Metabolism, Adv. Funct. Mater. 28 (2018) 1802793. doi:10.1002/adfm.201802793.
[151] R. Koivunen, E. Jutila, R. Bollström, P. Gane, Hydrophobic patterning of functional porous pigment coatings by inkjet printing, Microfluid. Nanofluidics. 20 (2016) 83. doi:10.1007/s10404-016-1747-9.
[152] E. Ollikainen, I. Lenic, T. Sikanen, Feasibility of Microchip Electrophoresis-Electrochemical Detection for Environmental Monitoring, Proc. 19th Int. Conf. Miniaturized Syst. Chem. Life Sci. (2015).
[153] FDA, U.S. Food and Drug Administration, Guidance for Industry – Bioanalytical Method Validation, (2001).

[154] S. Tuomikoski, T. Sikanen, R.A. Ketola, R. Kostiainen, T. Kotiaho, S. Franssila, Fabrication of enclosed SU-8 tips for electrospray ionization-mass spectrometry, Electrophoresis. 26 (2005) 4691–4702. doi:10.1002/elps.200500475.
[155] W.H.D. Jong, P.J. Borm, Drug delivery and nanoparticles: Applications and hazards, Int. J. Nanomedicine. 3 (2008) 133–149. doi:10.2147/IJN.S596.
[156] S. Naahidi, M. Jafari, F. Edalat, K. Raymond, A. Khademhosseini, P. Chen, Biocompatibility of engineered nanoparticles for drug delivery, J. Controlled Release. 166 (2013) 182–194. doi:10.1016/j.jconrel.2012.12.013.
[157] L.M. Bimbo, M. Sarparanta, H.A. Santos, A.J. Airaksinen, E. Mäkilä, T. Laaksonen, L. Peltonen, V.-P. Lehto, J. Hirvonen, J. Salonen, Biocompatibility of Thermally Hydrocarbonized Porous Silicon Nanoparticles and their Biodistribution in Rats, ACS Nano. 4 (2010) 3023–3032. doi:10.1021/nn901657w.
[158] N.M. Midde, S. Kumar, Development of NanoART for HIV treatment: minding the cytochrome P450 (CYP) enzymes, J Nanomed. 1 (2015) 24–32.
[159] E. Ollikainen, D. Liu, A. Kallio, E. Mäkilä, H. Zhang, J. Salonen, H.A. Santos, T.M. Sikanen, The impact of porous silicon nanoparticles on human cytochrome P450 metabolism in human liver microsomes in vitro, Eur. J. Pharm. Sci. 104 (2017) 124–132. doi:10.1016/j.ejps.2017.03.039.
[160] S.C. Gay, A.G. Roberts, J.R. Halpert, Structural Features of Cytochromes P450 and Ligands that Affect Drug Metabolism as Revealed by X-ray Crystallography and NMR, Future Med. Chem. 2 (2010) 1451–1468.
[161] D.M. Stresser, S.D. Turner, A.P. Blanchard, V.P. Miller, C.L. Crespi, Cytochrome P450 Fluorometric Substrates: Identification of Isoform-Selective Probes for Rat CYP2D2 and Human CYP3A4., Drug Metab. Dispos. 30 (2002) 845–852. doi:10.1124/dmd.30.7.845.
[162] L.H. Cohen, M.J. Remley, D. Raunig, A.D.N. Vaz, In Vitro Drug Interactions of Cytochrome P450: An Evaluation of Fluorogenic to Conventional Substrates, Drug Metab. Dispos. 31 (2003) 1005–1015. doi:10.1124/dmd.31.8.1005.
[163] M.T. Donato, N. Jiménez, J.V. Castell, M.J. Gómez-Lechón, Fluorescence-Based Assays for Screening Nine Cytochrome P450 (p450) Activities in Intact Cells Expressing Individual Human P450 Enzymes, Drug Metab. Dispos. 32 (2004) 699–706. doi:10.1124/dmd.32.7.699.
[164] N. Chauret, A. Gauthier, D.A. Nicoll-Griffith, Effect of common organic solvents on in vitro cytochrome P450-mediated metabolic activities in human liver microsomes, Drug Metab. Dispos. Biol. Fate Chem. 26 (1998) 1–4.
[165] A. Ghosal, N. Hapangama, Y. Yuan, X. Lu, D. Horne, J.E. Patrick, S. Zbaida, Rapid determination of enzyme activities of recombinant human cytochromes P450, human liver microsomes and hepatocytes, Biopharm. Drug Dispos. 24 (2003) 375–384. doi:10.1002/bdd.374.
[166] R. Yuan, S. Madani, X.-X. Wei, K. Reynolds, S.-M. Huang, Evaluation of Cytochrome P450 Probe Substrates Commonly Used by the Pharmaceutical Industry to Study in Vitro Drug Interactions, Drug Metab. Dispos. 30 (2002) 1311–1319. doi:10.1124/dmd.30.12.1311.
[167] L. Bell, S. Bickford, P.H. Nguyen, J. Wang, T. He, B. Zhang, Y. Friche, A. Zimmerlin, L. Urban, D. Bojanic, Evaluation of Fluorescence- and Mass Spectrometry—Based CYP Inhibition Assays for Use in Drug Discovery, J. Biomol. Screen. 13 (2008) 343–353. doi:10.1177/1087057108317480.
[168] P. Cohen, The role of protein phosphorylation in human health and disease., Eur. J. Biochem. 268 (2001) 5001–5010. doi:10.1046/j.0014-2956.2001.02473.x.
[169] Olsen George D., Morphine binding to human plasma proteins, Clin. Pharmacol. Ther. 17 (1975) 31–35. doi:10.1002/cpt197517131.

[170] E. Ollikainen, T. Aitta-aho, M. Koburg, R. Kostiainen, T. Sikanen, Rapid analysis of intraperitoneally administered morphine in mouse plasma and brain by microchip electrophoresis-electrochemical detection, Sci. Rep. 9 (2019) 3311. doi:10.1038/s41598-019-40116-5.
[171] M. Handal, M. Grung, S. Skurtveit, Å. Ripel, J. Mørland, Pharmacokinetic differences of morphine and morphine-glucuronides are reflected in locomotor activity, Pharmacol. Biochem. Behav. 73 (2002) 883–892. doi:10.1016/S0091-3057(02)00925-5.
[172] E. Ollikainen, A. Bonabi, N. Nordman, V. Jokinen, T. Kotiaho, R. Kostiainen, T. Sikanen, Rapid separation of phosphopeptides by microchip electrophoresis–electrospray ionization mass spectrometry, J. Chromatogr. A. 1440 (2016) 249–254. doi:10.1016/j.chroma.2016.02.063.
[173] EUNCL | Nanomedicine Characterisation Laboratory. http://www.euncl.eu/ (accessed May 8, 2019).
[174] J. Zhou, Q. Wen, S.-F. Li, Y.-F. Zhang, N. Gao, X. Tian, Y. Fang, J. Gao, M.-Z. Cui, X.-P. He, L.-J. Jia, H. Jin, H.-L. Qiao, Significant change of cytochrome P450s activities in patients with hepatocellular carcinoma, Oncotarget. 7 (2016) 50612–50623. doi:10.18632/oncotarget.9437.